



Cesium Ion Exchange Using Crystalline Silicotitanate with 5.6 M Sodium Simulant

July 2018

SK Fiskum
HA Colburn
RA Peterson

AM Rovira
MR Smoot

DISCLAIMER

This report was prepared as an account of work sponsored by an agency of the United States Government. Neither the United States Government nor any agency thereof, nor Battelle Memorial Institute, nor any of their employees, makes **any warranty, express or implied, or assumes any legal liability or responsibility for the accuracy, completeness, or usefulness of any information, apparatus, product, or process disclosed, or represents that its use would not infringe privately owned rights.** Reference herein to any specific commercial product, process, or service by trade name, trademark, manufacturer, or otherwise does not necessarily constitute or imply its endorsement, recommendation, or favoring by the United States Government or any agency thereof, or Battelle Memorial Institute. The views and opinions of authors expressed herein do not necessarily state or reflect those of the United States Government or any agency thereof.

PACIFIC NORTHWEST NATIONAL LABORATORY
operated by
BATTELLE
for the
UNITED STATES DEPARTMENT OF ENERGY
under Contract DE-AC05-76RL01830

Printed in the United States of America

Available to DOE and DOE contractors from the
Office of Scientific and Technical Information,
P.O. Box 62, Oak Ridge, TN 37831-0062;
ph: (865) 576-8401
fax: (865) 576-5728
email: reports@adonis.osti.gov

Available to the public from the National Technical Information Service
5301 Shawnee Rd., Alexandria, VA 22312
ph: (800) 553-NTIS (6847)
email: orders@ntis.gov <<http://www.ntis.gov/about/form.aspx>>
Online ordering: <http://www.ntis.gov>



This document was printed on recycled paper.

(8/2010)

Cesium Ion Exchange Using Crystalline Silicotitanate with 5.6 M Sodium Simulant

SK Fiskum
HA Colburn
RA Peterson

AM Rovira
MR Smoot

July 2018

Prepared for
the U.S. Department of Energy
under Contract DE-AC05-76RL01830

Pacific Northwest National Laboratory
Richland, Washington 99352

Executive Summary

The Low-Activity Waste Pretreatment System (LAWPS) facility is planned to pretreat Hanford tank waste supernate by filtering to remove solids and processing through ion exchange columns to remove cesium. The ion exchange media is currently (since 2018) targeted to be crystalline silicotitanate (CST). This material has been produced as an engineered form (generally spherical beads) by Honeywell UOP LLC (Des Plaines, IL). Previous forms of this media have been tested in a wide array of simulants and process scales, but column breakthrough and batch contact testing to date on actual tank waste has been limited to a few tank wastes. Washington River Protection Solutions requested a series of studies to demonstrate Cs load behavior in a small column format and determine if a simple batch contact test with CST can be used to qualify tank waste supernate prior to processing it in the LAWPS. The goal of the batch contact testing is to determine if there are any issues with the tank waste that would preclude Cs removal by the ion exchanger.

Testing was conducted with IONSIV™ R9140-B CST provided by Honeywell UOP in 2018 (Batch 2081000057). The CST was received in the sodium (Na) form, so no pretreatment conditioning to convert to the Na form was required. Before use in testing, the CST was passed through a #25 sieve (710-micron openings) and collected on a #60 sieve (250-micron openings) with the intent of removing any large and fine particles. Physical properties were measured on the CST including particle size distribution ($d_{50} = 570$ microns) and scanning electron micrographic examination. The CST was rinsed with water until the contact solution was visually nearly clear. The CST bed density (1.00 g/mL) and CST bed void fraction (0.656) were measured on the sieved and rinsed CST.

The batch contact testing varied Cs concentration in a 5.6 M Na simple simulant solution. Testing was conducted in a liquid volume to solids mass ratio of 200. The distribution coefficient (K_d) was determined to be 770 mL/g at the Cs equilibrium condition of 8.0 $\mu\text{g/mL}$; with a bed density of 1.00 g/mL, this corresponds to a predicted 50% Cs breakthrough of 770 bed volumes (BVs). The Cs load capacity at 8.0 $\mu\text{g/mL}$ equilibrium condition was determined to be 6.16 mg Cs/g dry CST.

The column testing was prototypic to the intended LAWPS operations in a lead-lag column format, albeit on a small-scale basis with 10-mL CST beds. The feed was processed downflow through the lead column and then through the lag column. Three flowrates were tested: 1.19, 1.99, and 4.56 BV/h. The feed was displaced with 0.1 M NaOH, and then the columns were rinsed with water sequentially through the lead then lag columns. One column system was evaluated top to bottom with a gamma scanner to assess the axial Cs loading. Table ES.1 summarizes the relevant Cs loading characteristics.

Table ES.1. Column Performance Summary with 5.6 M Na Simple Simulant

Flowrate	50% Cs Breakthrough, BV	Cs Loading Capacity, mg/g	Lag Column Contract Limit ^(a) Breakthrough, BV
1.19 BV/h	800	6.61	590
1.99 BV/h	800	6.38	475
4.56 BV/h	690	6.03	260

(a) The contract limit is defined to be 0.114 %C/C₀, congruent with tank waste at 5.6 M Na and 156 μCi/mL ¹³⁷Cs. This corresponds to a decontamination factor of 878.

The predicted 50% Cs breakthrough determined from batch contact results agreed within 10% of the column results. The capacity determined from batch contact testing agreed with column testing within 7%. It is not possible to equate the batch contact results to understanding the number of BVs that can be processed before reaching the contract limit for Cs from the lag column, as this depends on the slope of the load curve/mass transfer zone.

Acknowledgments

The authors thank the ASO count room staff Truc Trang-Le and Mike Cantaloub for rapid ^{137}Cs analysis for the batch contact and column load/elution sample analysis. We thank Edgar Buck for scanning electron micrographs and analysis and Carlyne Burns for particle size distribution measurements. We thank Renee Russell for carefully reviewing the ion exchange calculation files, test data packages, and this technical report. We thank Matt Wilburn for his editorial review.

Acronyms and Abbreviations

ASO	Analytical Support Operations
ASR	Analytical Service Request
BV	bed volume
CST	crystalline silicotitanate
DI	deionized
DSSF	double-shell slurry feed
FMI	Fluid Metering, Inc.
GEA	gamma energy analysis
LAW	low-activity waste
LAWPS	Low-Activity Waste Pretreatment System
PNNL	Pacific Northwest National Laboratory
PSD	particle size distribution
SwRI	Southwest Research Institute
TRL	technical readiness level
WRPS	Washington River Protection Solutions
WTP	Hanford Tank Waste Treatment and Immobilization Plant

Contents

Executive Summary	ii
Acknowledgments.....	iv
Acronyms and Abbreviations	v
1.0 Introduction	1.1
2.0 Test Conditions.....	2.1
2.1 CST Media	2.1
2.2 Ion Exchange Process Feed.....	2.3
2.3 Batch Contact Conditions.....	2.4
2.3.1 Batch Contact Sample Preparation.....	2.5
2.3.2 Batch Contact Analysis and Calculations	2.6
2.4 Ion Exchange Process Testing.....	2.7
2.4.1 Ion Exchange Column System	2.7
2.4.2 Bed Volume and System Volume	2.10
2.4.3 CST Bed Pretreatment.....	2.10
2.4.4 5.6 M Na Simple Simulant Process Conditions	2.10
2.5 Sample Analysis.....	2.14
3.0 Batch Contact Results.....	3.1
3.1 5.6 M Na Simulant Batch Contact Results.....	3.1
4.0 Column Test Results.....	4.1
4.1 Cs Load, Feed Displacement, and Water Rinse Results	4.1
4.2 Column Gamma Scan.....	4.5
4.3 Cesium Activity Balance from Ion Exchange Processing.....	4.6
4.4 Measured and Predicted 50% Cs Breakthrough.....	4.8
4.5 Contract Limit	4.9
4.6 Transition Zone	4.12
5.0 Conclusions and Recommendations	5.1
5.1 Physical Properties	5.1
5.2 Batch Contact Testing	5.1
5.3 Column Testing.....	5.1
5.4 Recommendations for Future Testing.....	5.2
6.0 References	6.1
Appendix A Column Load and Rinse Data	A.1

Figures

Figure 2.1. PSD of CST Media, IONSIV™ R9140-B, Batch 2081000057, As-received (AR) and After Sieving (SC)	2.2
Figure 2.2. Ion Exchange System Schematic.....	2.8
Figure 2.3. CST Bed Supports with Centimeter Scale.....	2.8
Figure 2.4. Ion Exchange Column Apparatus in the Fume Hood.....	2.9
Figure 2.5. Red Columns a) Lead and b) Lag following Load Step Showing Slight Discoloration on Top of Lead Column.....	2.12
Figure 2.6. Drained Fluids from the Blue Lead and Lag Columns Showing Sediment from Lead Column	2.13
Figure 2.7. Axial Gamma Scan Analysis System	2.14
Figure 3.1. Equilibrium Cs K_d Curve for 5.6 M Na Simple Simulant with CST.....	3.2
Figure 3.2. Comparison of Current Test (24-hour Contact Time) with Brown et al. (1996) Data	3.2
Figure 3.3. Isotherm for the 5.6 M Na Simple Simulant with CST	3.3
Figure 4.1. Lead and Lag Column Cs Load Profiles of 5.6 M Na Simple Simulant with 8.0 $\mu\text{g/mL}$ Cs at 1.19 BV/h (a) Linear-Linear Plot, (b) Probability-Linear Plot	4.2
Figure 4.2. Lead and Lag Column Cs Load Profiles of 5.6 M Na Simple Simulant with 8.0 $\mu\text{g/mL}$ Cs at 1.99 BV/h (a) Linear-Linear Plot, (b) Probability-Linear Plot	4.3
Figure 4.3. Lead and Lag Column Cs Load Profiles of 5.6 M Na Simple Simulant with 8.0 $\mu\text{g/mL}$ Cs at 4.56 BV/h (a) Linear-Linear Plot, (b) Probability-Linear Plot	4.4
Figure 4.4. Lead and Lag Blue Column System Gamma Scans Showing Relative ^{137}Cs Activity.....	4.5
Figure 4.5. Lead Column Comparison.....	4.9
Figure 4.6. Comparison of Lag Column Performance.....	4.10
Figure 4.7. Volume Processed to Reach Contract Limit vs. Flowrate.....	4.11
Figure 4.8. Cs Load Profiles at Two Different Linear Velocities and Nearly Constant Residence Time	4.12

Tables

Table 2.1. Cumulative Particle Undersize Fractions for R9140-B CST	2.1
Table 2.2. Washed R9140-B, Batch 2081000057, CST Physical Properties.....	2.3
Table 2.3. 5.6 M Na Simple Simulant Composition.....	2.4
Table 2.4. Initial Cs Concentrations Used for the 5.6 M Na Simple Simulant Batch Contact Tests	2.5
Table 2.5. Experimental Conditions for the Red Column, 1.19 BV/h.....	2.11
Table 2.6. Experimental Conditions for the Blue Column, 1.99 BV/h.....	2.11
Table 2.7. Experimental Conditions for the Green Column, 4.56 BV/h.....	2.11
Table 3.1. Equilibrium Results for Batch Contact Samples in 5.6 M Na Simple Simulant.....	3.1
Table 4.1. ¹³⁷ Cs Activity Balance for the Red Column Test.....	4.6
Table 4.2. ¹³⁷ Cs Activity Balance for the Blue Column Test.....	4.7
Table 4.3. ¹³⁷ Cs Activity Balance for the Green Column Test.....	4.7
Table 4.4. Cs Capacity in CST.....	4.8
Table 4.5. Bed Volumes Processed to Reach Contract Limit.....	4.10
Table 4.6. Flowrate Effect on the Transition Zone	4.13
Table 5.1. Column Performance Summary with 5.6 M Na Simple Simulant.....	5.2

1.0 Introduction

Initial processing to filter and remove cesium (Cs) from Hanford tank waste supernate will be conducted to expedite delivery of the tank waste to the Hanford Tank Waste Treatment and Immobilization Plant (WTP) Low-Activity Waste (LAW) Facility. Tank waste supernatant will be transferred from a Hanford staging tank and then pretreated in the Low-Activity Waste Pretreatment System (LAWPS) to meet the WTP LAW Facility waste acceptance criteria.¹ Specific to ¹³⁷Cs, the WTP requires < 3.18E-5 Ci ¹³⁷Cs/mole of Na (contract limit). The key process operations for treating the waste include solids filtration and Cs removal. At the LAWPS, Cs removal is planned to be accomplished by ion exchange. Spherical resorcinol-formaldehyde ion exchange resin had been tested to support this effort. However, emphasis was shifted to the use of crystalline silicotitanate (CST), manufactured in a granular, nominally spherical (engineered) form by Honeywell UOP LLC (Des Plaines, IL).

Several studies of CST for Cs removal from high salt waste have been described (Brown et al. 1996; Hendrickson et al. 1996; Walker et al. 1999; King 2007). The ion exchange performance of supernatant feed on CST has been modeled (Hamm et al. 2002). These studies show great promise for the CST use on Hanford tank waste supernate. The use of CST include issues with column plugging, the unknown fate of other elements (such as Pu) during ion exchange, and the untested general applicability to the wide range of Hanford tank waste.

Honeywell UOP LLC has also modified the CST formulation since earlier studies conducted largely in the 1990s. The CST modifications were proprietary but revolved around mitigating the column plugging and CST clumping. Limited information is available with the current production CST material on actual Hanford tank waste and simulants.

This study is intended to investigate the Cs exchange performance of CST as currently produced by Honeywell UOP LLC. Testing included 1) batch contact testing with CST to determine the Cs distribution coefficient (K_d) and load capacity in the 5.6 M Na simple simulant matrix and 2) evaluation of Cs load curves as a function of flowrate on small column CST beds. The batch contact testing is of particular interest by LAWPS for use in feed qualification for ion exchange. The idea is to determine if the small-scale, rapid batch contact test can be used to verify applicability of a particular feed to successful Cs removal by the cesium ion exchange unit operation.

This report discusses results of batch contact and column testing studies from testing 5.6 M Na simple simulant with 8.0 µg/mL Cs. Column testing was conducted at three different flowrates on dual column systems. The efficacy of using the batch contact testing to predict column performance is discussed. Results of the small-scale column simulant testing can be compared to full-scale simulant testing in future studies.

¹ 24590-WTP-ICD-MG-01-030. 2015. *ICD 30 – Interface Control Document for Direct LAW Feed*. Bechtel National, Inc., Richland, Washington.

2.0 Test Conditions

This section describes the CST media, 5.6 M Na simple simulant, batch contact test conditions, and column ion exchange test conditions. All testing was conducted in accordance with a test plan prepared by Pacific Northwest National Laboratory (PNNL) and approved by Washington River Protection Solutions (WRPS).¹

2.1 CST Media

PNNL and WRPS worked with UOP LLC (Honeywell Company, Des Plaines, IL) to receive proprietary samples of CST selective media. One each 3-kilogram samples of IONSIV™ R9140-B, Batch 2081000057, and IONSIV™ R9120-B, Batch 2081000001, were received at PNNL for testing on February 26, 2018. Both materials were in the bead form. Sample R9140-B was provided in the sodium form with an indicated² mesh size of -30/+60. Sample R9120-B was provided in the hydrogen form with a specified mesh size of -20/+40. Because the test columns were narrow (1.4 cm inside diameter), the smaller sieve fraction material, R9140-B, was chosen for testing. This also precluded the need for pretreatment to convert it to the sodium form.

A CST subsample was collected with a cone penetrometer. Repeated plunges with the cone penetrometer were conducted in order to obtain enough material for testing. A bead of CST was placed on a balance and pressed with the flat end of a spatula. The bead crushed easily with <100 g force to a powder consistency; this characteristic should be accounted for when collecting CST subsamples from the bulk container and post-tested columns. The bulk density of as-received CST was measured at 1.07 g/mL. A subsample was submitted for particle size distribution (PSD) analysis, which was conducted using a Malvern Mastersizer 2000 with water as the suspension medium. Results are shown in Table 2.1 and Figure 2.1. The PSD was tight, ranging from 419 to 779 microns (D10 to D90). The PSD did not match the expected -30/+60 mesh size (250-600 microns) but was more consistent with a -20/+40 mesh size (425-850 microns).

Table 2.1. Cumulative Particle Undersize Fractions for R9140-B CST

	R9140-B, As-Received	R9140-B, Sieved
D10	419	418
D50	573	571
D90	779	775

¹ TP-DFTP-029, Rev.0.0. *DFLAW Test Platform Cesium Ion Exchange Testing with AP-107 Tank Waste and 5.6 M Na Simple Simulant*. Pacific Northwest National Laboratory, Richland Washington. 2017.

² Per email from Matt Landon (WRPS) to Jim Szczurek (Honeywell UOP LLC), January 31, 2018, subject line: ION EXCHANGE MEDIA UOP HONEYWELL.

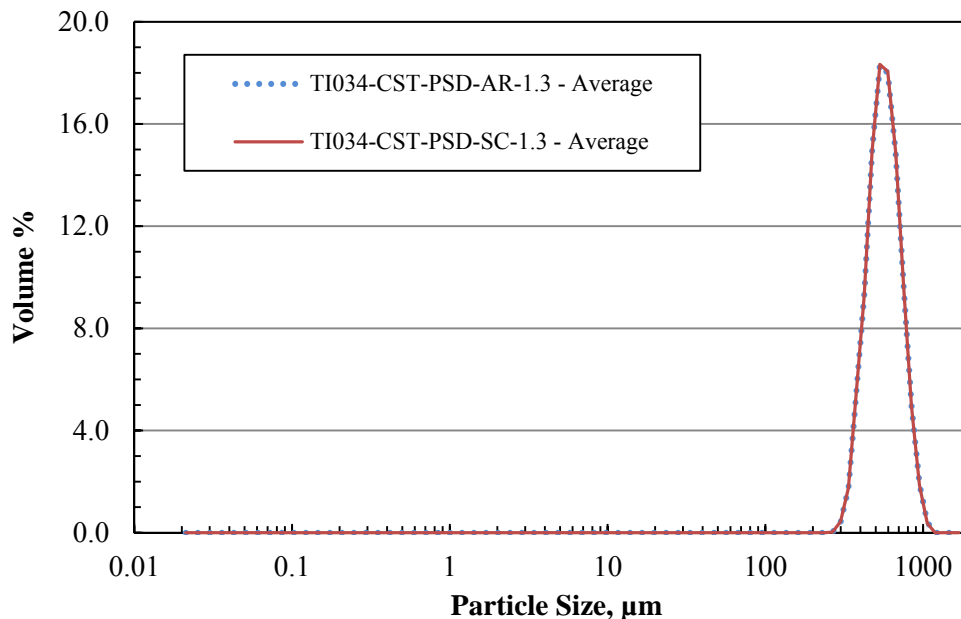


Figure 2.1. PSD of CST Media, IONSIV™ R9140-B, Batch 2081000057, As-received (AR) and After Sieving (SC)

Scanning electron micrographs of the CST, as-received, were collected.¹ The particles were generally spherical with diameters around 560 to 630 micrometers. The particle surface was rough and fracture lines were evident in several of the particles. Energy dispersive spectroscopy indicated that the beads contained oxygen, titanium, zirconium, niobium, sodium, and silicon.

The CST subsample was passed through a 25 mesh sieve (ASTM E11). It was important to remove large particle material to create a more uniform ion exchange bed and mitigate the potential for wall effects (Harland 1994) from large particles. A 30 mesh sieve was initially used to remove large particles, but it was quickly blinded. The mass fraction retained on the 25 mesh sieve was 7.7 wt%. The CST was also collected on a 60 mesh sieve (ASTM E11). Column plugging had been reported previously (Rapko et al. 2005; Walker et al. 1999), and it was important to remove any fines that may fill interstitial spaces and result in plugging. The mass fraction passing through the 60 mesh sieve was 1.7 wt%. The bulk density of the sieve fraction was measured in duplicate at 1.03 and 1.06 g/mL. A subsample was submitted for PSD analysis (Figure 2.1). There was no observable shift in the PSD from before and after sieving, despite the fact that the tails (+25 mesh and -60 mesh) were removed. The small volume fraction removed (both the fines and the large particles) were either inconsequential to the total volume fraction analysis and/or the removed fractions counterbalanced each other causing no shift to the peak. Data in Table 2.1 and the traces in Figure 2.1 show the sieved CST PSD to be virtually identical to the unseived CST PSD.

The -25/+60 mesh sieved material was subsequently washed with water. Nominally one volume CST was contacted with two volumes deionized water. This was repeated seven times, at which point the contacted water was fairly, though not completely, clear. The wash water was initially opaque. After standing overnight, opacity was still evident with minimal solids settling. The combined water washes were dried

¹ SEM images will be maintained in the project record should the need arise to compare pre- and post-tested CST morphology.

to constant mass at 100 °C to assess the suspended solids mass content. The fines removed during water washing constituted 0.38 wt% of the sampled aliquot (dry mass basis).

Duplicate 10-mL fractions of the sieved and washed CST were dried overnight in air at room temperature to remove all interstitial water. The dried CST mass and settled volume in a 10-mL graduated cylinder were measured to determine bulk density. The dried CST was then added slowly to a known volume and mass of deionized water in a 25-mL graduated cylinder. Effervescence was noted upon initial contact with water. The CST was gently mixed by turning the graduated cylinder, allowing free release of the gas. The cylinder was tapped until the CST reached constant volume. The total slurry volume and settled CST bed volume (BV) were measured. The net CST volume (not including the bed void volume) was calculated from the water displacement. The water above the CST bed was removed and the net CST plus water mass was calculated. The dry CST mass was subtracted from net mass to determine the interstitial water mass (and volume). Table 2.2 summarizes the physical properties of the washed CST that was loaded into the ion exchange columns and used for batch contacts.

Table 2.2. Washed R9140-B, Batch 2081000057, CST Physical Properties

Parameter	Sample 1	Sample 2
Dry CST mass, g	9.8728	9.8616
Dry CST bulk volume, mL	10.0	9.7
Bulk density, g/mL	0.987	1.02
Water displacement volume, mL	3.3	3.3
Wet CST bed volume, mL	10.0	9.8
CST bed density, g/mL	0.987	1.01
Settled bed void volume, %	65.6	65.6

2.2 Ion Exchange Process Feed

A total of 40 L of the 5.6 M Na simple simulant was prepared by Noah Technologies Inc. (San Antonio, Texas). The preparation was conducted as defined by Russell et al. (2017), with the exception that Cs concentration was decreased from 14 to 8.0 µg/mL and sodium oxalate was completely omitted to preclude the presence of undissolved solids. Component salts were American Chemical Society Reagent Grade or similar with ≥99.1 % purity. The measured component masses and calculated ionic species concentrations are provided in Table 2.3. All components dissolved.

Table 2.3. 5.6 M Na Simple Simulant Composition

Component	Component FW, g/mole	Measured Component Mass, g	Ionic Species	Calculated Species Conc., M	Measured Species Conc., M ^(a)	Measured / Expected
Al(NO ₃) ₃ •9H ₂ O	375.15	2511	Al(OH) ₄ ⁻	0.166	0.145	0.87
NaOH (50% w/w)	40.00	6663	free OH ⁻	1.41	1.37	0.97
CsNO ₃	194.91	0.468	Cs ⁺	6.00E-5	5.99E-5 ^(b)	1.00
KCl	74.55	367	K ⁺ and Cl ⁻	0.122	0.102	0.84
Na ₂ SO ₄	142.05	376	SO ₄ ²⁻	0.0660	0.0582	0.88
NaNO ₂	69.00	2829	NO ₂ ⁻	1.02	0.915	0.90
NaNO ₃	85.00	4372	NO ₃ ⁻	1.78	1.55	0.87
Na ₃ PO ₄ -12H ₂ O	380.13	657	PO ₄ ³⁻	0.0434	0.0433	1.00
Na ₂ CO ₃ -H ₂ O	124.00	2316	CO ₃ ²⁻	0.468	0.391	0.84
Deionized water	18.02	29,908	Na ⁺	5.57	4.81	0.86

(a) Analysis was conducted by SwRI, San Antonio, Texas.

(b) Measured at PNNL per ASR 0457. The Cs measured by SwRI was 84% of target, indicating a low analytical bias. The PNNL measurement agreed with the target makeup value of 8.0 µg/mL.

FW = formula weight

Analysis was conducted by Southwest Research Institute (SwRI, San Antonio, Texas); PNNL staff measured the ¹³³Cs by inductively coupled plasma mass spectrometry according to Analytical Service Request (ASR) 0457. Analysis results agreed with the preparation formulation within 84% to 100%. The solution density, 1.247 g/mL, was slightly below the target 1.26 g/mL reported by Russell et al. (2017). The simulant preparation was considered accurate.

Multiple 4-L aliquots of the simple simulant were spiked with 210 µCi ¹³⁷Cs tracer (February 2018 reference date) to support both the batch contact and column testing. The total Cs concentration in the tracer (from the carrier Cs and ¹³⁷Cs) was inconsequential to the prepared 8.0 µg/mL Cs concentration. The tracer was allowed to equilibrate with the native Cs ~16 hours or more before processing.

2.3 Batch Contact Conditions

Batch-distribution contact testing is a rapid method for determining relative equilibrium performance of ion exchange materials in a given matrix. Batch contact solutions consist of the target test matrix plus various amounts of added ¹³³Cs. The equilibrium Cs concentrations are determined after batch contacts to assess Cs loading capacity on the CST and the Cs distribution coefficient (K_d) under nominal process conditions. The preparations and batch contacts were processed in accordance with a test instruction¹ (prepared and approved internally) and as described in the following subsections.

¹ Fiskum SK. 2018. TI-DFTP-035, *Batch Contacts with Crystalline Silicotitanate in 5.6 M Na Simple Simulant Matrix*. Pacific Northwest National Laboratory, Richland, Washington. Issued February 2018.

2.3.1 Batch Contact Sample Preparation

Two Cs spike solutions (140 mg/mL and 14.0 mg/mL) were prepared by dissolving CsNO₃ (99.99%, Johnson Matthey, Lot G14013) in water. Small volumes (0.1 to 0.6 mL) of the Cs spike solutions were added to three stock containers. The highest concentration Cs was added by directly weighing CsNO₃ crystals into a fourth container. (Minimizing the added spike volume minimizes matrix dilution [distortion] such that the batch contact matrix best matches the matrix processed through the ion exchange columns.) The 5.6 M Na simple simulant, containing 8.0 µg/mL Cs, was initially spiked with ¹³⁷Cs tracer at 0.05 µCi/mL.¹ Approximately 45-mL aliquots of this solution were transferred to each of the Cs spike solution containers. All Cs spike transfers and 5.6 M Na simple simulant transfers were tracked by mass and actual volume deliveries calculated based on mass and solution density. Table 2.4 shows the calculated initial Cs concentrations in the batch contact stock solutions.

Table 2.4. Initial Cs Concentrations Used for the 5.6 M Na Simple Simulant Batch Contact Tests

Solution ID	Cs Concentration, mg/L	Cs Concentration, Molarity
TI-035-S0	8.0	6.02E-5
TI-035-S1	39.1	2.94E-4
TI-035-S2	199	1.49E-3
TI-035-S3	930	7.00E-3
TI-035-S4	6152	4.63E-2

An aliquot of the washed CST was collected and placed in a beaker. It was air dried at room temperature to remove bulk water. Once the CST was free flowing, it was transferred to a vial and capped. An aliquot of CST was removed to determine the remaining water content in the CST (nominal F-factor evaluation) and the vial containing the remaining partially dried CST was held in reserve. The F-factor sample aliquot was dried at ~95 °C overnight to determine the nominal water content remaining in the partially dried CST. This nominal F-factor was used to determine the target CST aliquot mass to collect for the batch contact samples. The partially dried CST contained about 17% water by mass.

A precisely weighed quantity (target of 0.126 g ± 1%) of the partially-dried CST was aliquoted into a 30-mL polyethylene bottle for each batch contact sample. The CST mass aliquot was targeted to achieve a phase ratio (volume of liquid to mass of dry CST) of 200. The batch contact tests were prepared in duplicate at each Cs concentration.

Two F-factor samples were also weighed (initial mass, M_I), one at the beginning of CST aliquoting process and one at the end of CST aliquoting process. The F-factor samples were dried to constant mass (final mass, M_F) at 100 °C to determine the dry CST mass. The F-factor was calculated according to Eq. (2.1). The average of the two F-factor samples was used to calculate the dry CST mass contacted with solution, as discussed in Section 2.3.2.

$$\frac{M_F}{M_I} = \text{F-Factor} \quad (2.1)$$

¹ The ¹³⁷Cs in the traced 5.6 M Na simple simulant was used to determine the Cs-exchange behavior in each sample using gamma energy analysis (GEA) as discussed in Section 2.3.2.

The CST aliquots were contacted with 20 mL of the various contact solutions (see Table 2.4). The solution volume was transferred by pipet; the actual contact solution volume was determined by mass difference and solution density. The targeted phase ratio (liquid volume to exchanger mass) was 200 mL/g. The obtained ratio varied between 180 and 193 mL/g.

The batch contact vials were placed upright in an IKA KS125 orbital shaker with 4-mm shaker diameter set to ~700 revolutions per minute. Rigorous mixing was observed for all samples; however, the CST remained on the floor of the poly bottle. A vial of water was incorporated with the set to act as a temperature sentinel. The CST primary samples were contacted for 24 hours and the duplicates were contacted for 45 hours. Equilibrium for the engineered CST had been confirmed to be reached within 24 hours (Brown et al. 1996); however, a check at longer (45-hour) contact time was deemed prudent. The temperature was not controlled. Half the samples were mixed for 24 hours; the temperature sentinel was 25 °C; the duplicate samples were mixed for 45 hours; the temperature sentinel was 24 °C. After contact, the CST was settled and the aqueous fractions were removed and filtered through 0.45- μ m pore size nylon-membrane syringe filters.

2.3.2 Batch Contact Analysis and Calculations

Filtered 2-mL aliquots were collected for GEA to determine the ^{137}Cs concentrations. Similarly, 2-mL aliquots of the parent (un-contacted) Cs-spiked solutions were collected for GEA. The ^{137}Cs tracer concentrations in aliquots of the un-contacted sample solutions were used to define the initial ^{137}Cs concentrations (C_0) for each test matrix. Final (equilibrium) Cs concentrations (C_{SEq}) were calculated relative to the ^{137}Cs recovered in the contacted samples (C_1) according to Eq. (2.2):

$$C_{S_0} \times \left(\frac{C_1}{C_0} \right) = C_{\text{SEq}} \quad (2.2)$$

where C_{S_0} = initial Cs concentration in solution ($\mu\text{g/mL}$ or M)

C_1 = equilibrium ^{137}Cs concentration in solution ($\mu\text{Ci/mL}$)

C_0 = initial ^{137}Cs concentration in solution ($\mu\text{Ci/mL}$)

C_{SEq} = equilibrium Cs concentration in solution ($\mu\text{g/mL}$ or M)

The equilibrium Cs concentrations loaded onto the CST (C_{SIX} in units of mg Cs per gram of dry CST mass) were calculated according to Eq. (2.3):

$$\frac{C_{S_0} \times V \times \left(1 - \frac{C_1}{C_0} \right)}{M \times F \times 1000} = C_{\text{SIX}} \quad (2.3)$$

where C_{SIX} = equilibrium Cs concentration in the CST (mg Cs/g CST)

C_{S_0} = initial Cs concentration in solution ($\mu\text{g/mL}$)

V = volume of the batch contact liquid (mL)

C_1 = final ^{137}Cs tracer concentration in solution ($\mu\text{Ci/mL}$)

C_0 = initial ^{137}Cs tracer concentration in solution ($\mu\text{Ci/mL}$)

M = mass of CST (g)

F = F-factor, mass of the dried CST divided by the mass of the undried CST
1000 = conversion factor to convert μg to mg

The Cs batch K_d values were determined according to the standard formula shown in Eq. (2.4):

$$\frac{(C_0 - C_1)}{C_1} \times \frac{V}{M \times F} = K_d \quad (2.4)$$

where C_0 = initial ^{137}Cs concentration ($\mu\text{Ci/mL}$)

C_1 = final (equilibrium) ^{137}Cs concentration ($\mu\text{Ci/mL}$)

V = volume of the batch contact liquid (mL)

M = mass of CST (g)

F = F-factor, mass of the dried CST divided by the mass of the undried CST

K_d = batch-distribution coefficient (mL/g)

Errors were kept small because ^{137}Cs tracer was used; samples with low ^{137}Cs concentrations were counted longer to reduce statistical counting error. Sample count errors were less than 1% ($1-\sigma$). Mass errors were less than 1%.

2.4 Ion Exchange Process Testing

This section describes the ion exchange column system and the process conditions. The preparations and column testing were conducted in accordance with a test instruction¹ (prepared and approved internally) and are described as follows.

2.4.1 Ion Exchange Column System

Three ion exchange systems were set up as shown schematically in Figure 2.2 (lead to lag solution flow). Each system consisted of two columns containing ion exchange media, a small metering pump, three valves, a pressure gauge, and a pressure-relief valve. The valves were three-way valves that could be turned to the flow position (upward) to flow solution through the entire system or a sample position (downward) to collect samples/fluids. Valve 1 was placed near the outlet of the pump and was used to isolate the column from the pump and collect initial fluids and to expel air from the lines at the initial setup. Valves 2 and 3 were primarily used to obtain samples and closed to isolate the system during storage periods.

¹ Fiskum SK. 2018. TI-DFTP-034, *Cesium Removal from 5.6 M Na Simple Simulant Using Crystalline Silicotitanate in Dual-Column Format at Three Flow Rates*. Pacific Northwest National Laboratory, Richland, Washington. Issued February 2018.

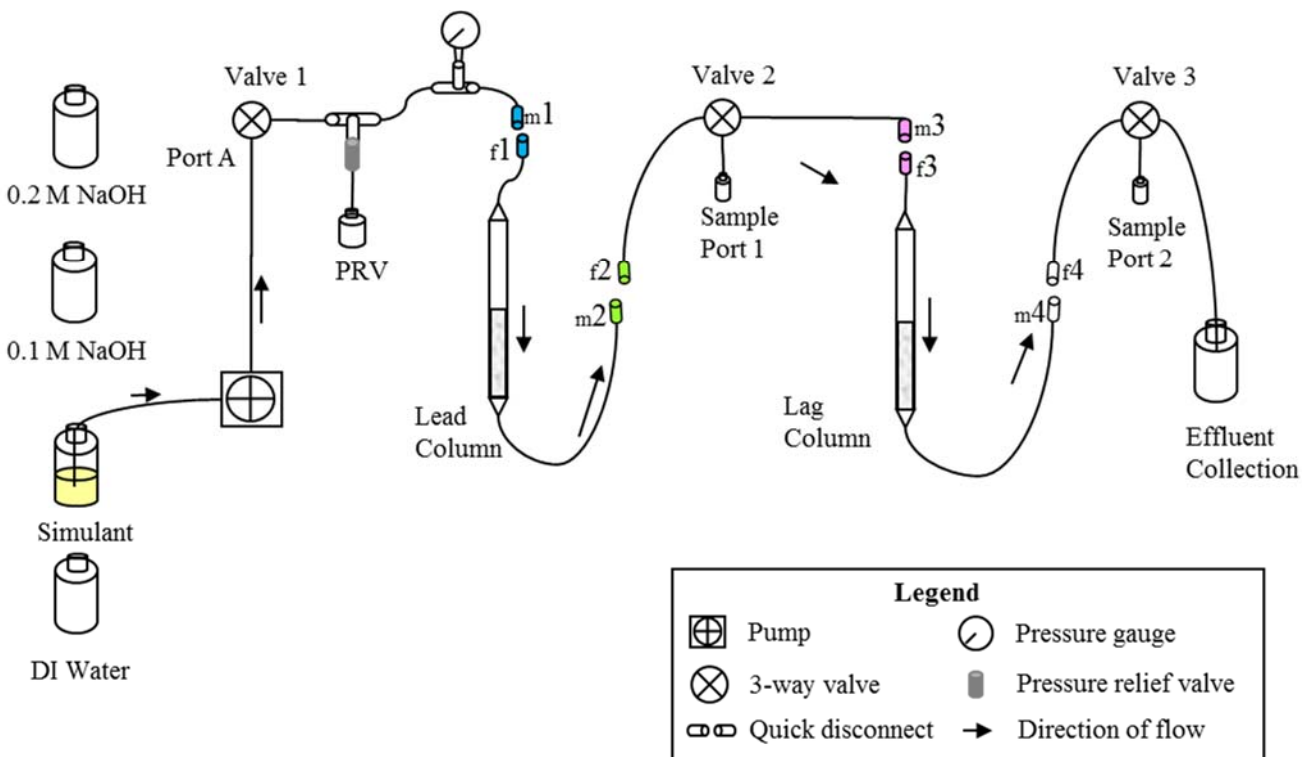


Figure 2.2. Ion Exchange System Schematic

Column assemblies were purchased from Spectrum Chromatography (Houston, TX), part number 125009. The column assembly included the column plus the top and bottom end fittings. Each column was made of borosilicate glass and was 20 cm tall with an inside diameter of 1.44 cm (corresponding to a CST volume of 1.67 mL/cm). Column fittings were composed of polytetrafluoroethylene (PTFE) and Teflon endplates and ferrule fittings for 1/8 in. outside diameter tubing.

Ion exchange bed supports were crafted in-house. They were made of stainless steel, 200 mesh screens tack welded onto stainless steel support rings. The support rings were stabilized with snug-fitting O-rings to remain stationary in the column once seated. Figure 2.3 shows replacement resin bed supports similar to those in the columns along with a centimeter scale. The resin bed supports were positioned just above the sight line of the lower column fitting.

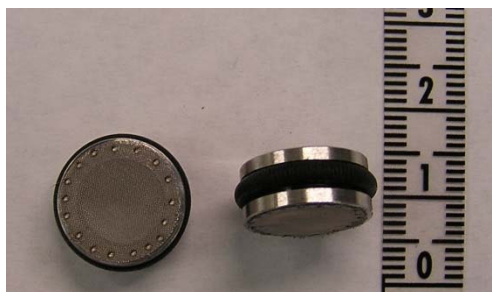


Figure 2.3. CST Bed Supports with Centimeter Scale

The cavity below the screen support was filled with 4-mm-diameter glass beads, reducing the fluid-filled volume from ~4 to ~2 mL. The height of the CST bed was measured with an adhesive millimeter-scale

scale affixed to the column with the zero point set to the top of the resin bed support. The associated height measurement error was estimated to be ± 2 mm.

Most of the connecting tubing was 1/8-in. outside diameter and 1/16-in. inside diameter and was made of polyethylene. The inlet sample line ended at the top column fitting. Tubing between the input of Valve 1 and the exit of the pressure gauge was 1/8-in. outside diameter stainless steel. The column assembly contained an in-line Swagelok Poppet pressure relief check valve with a 10-psi trigger (Solon, OH) and a 15-psi pressure gauge (Swagelok). Valved quick-disconnects (Cole Parmer, Vernon Hills, IL) were installed in-line to ease column removal and switching. Fluid Metering, Inc. (FMI) QVG50 pumps (Syosset, NY) equipped with a ceramic and Kynar[®] coated low-flow piston pump heads were used to introduce all fluids. The flowrate was controlled with a remotely operated FMI stroke-rate controller. The pump was set up to deliver flowrates from 0.2 to 0.8 mL/min. The actual volume pumped was determined using the mass of the fluid collected divided by the fluid density. The holdup volume of the entire ion exchange system, ~48 mL, was the summed volume of all fluid-filled parts.

Two manifold assemblies were prepared; one system was used sequentially to test two different flowrates. The columns were color coded for ease of operation and data recording; the Red columns processed 1.19 BV/h; the Blue columns processed 1.99 BV/h, and the Green processed 4.56 BV/h. Figure 2.4 is a photograph of the Red column assembly. The lead column is on the left and the lag column on the right. The Green system used the same manifold following completion of the Blue system test. The CST beds were 6 cm tall. The fluid height was set at nominally 12 cm, or 1 BV above the CST bed. The pump and columns were suspended over secondary containment. The pressure-relief valve was plumbed to a collection bottle capable of collecting an entire shift's worth of process fluid, should the column system plug.

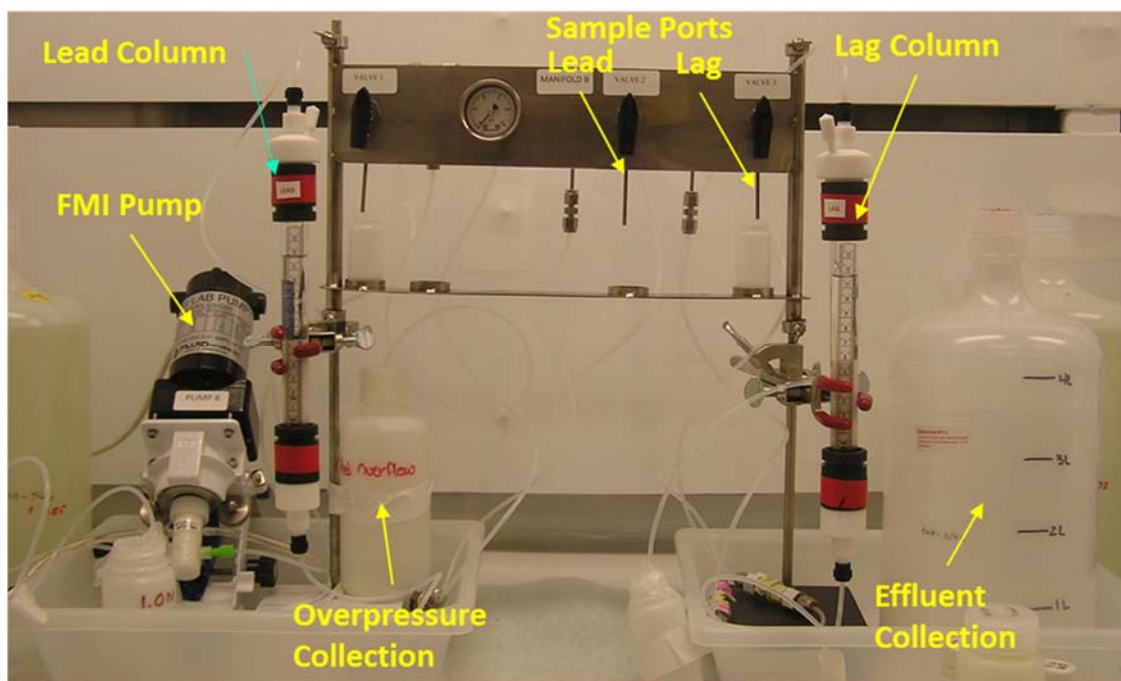


Figure 2.4. Ion Exchange Column Apparatus in the Fume Hood

After loading the CST into the columns, the system was pressure tested to assess and fix potential leaks. In one case, upon release of the pressure, bubbles were observed in the CST bed. In this case, the CST was removed and repacked.

2.4.2 Bed Volume and System Volume

The CST BV was defined as the volume of the sieved and washed CST bed as measured in a graduated cylinder before transfer to the ion exchange column; the CST bed included interstitial water. The graduated cylinder was tapped with a rubber bung to settle the CST bed to its smallest volume. The lead and lag column BVs were measured at 10.0 mL in this manner. The CST did not change volume during processing steps.

The system volume was defined as the combined lead and lag column CST BVs, i.e., 20 mL. System volume assessments are discussed in Section 4.5.

2.4.3 CST Bed Pretreatment

The in-column CST pretreatment simply constituted an initial system flush with 50 to 60 mL 0.2 M NaOH; this concentration was lower than the targeted concentration of 1.0 M due to a preparation error. The volume processed was essentially 1.4 times the total fluidic volume in the system. Because the CST was obtained from the vendor as the pretreated Na form, no further conditioning was deemed necessary. The conversion of the fluidic volume to strong base precludes the potential for aluminum in the simulant to precipitate as $\text{Al}(\text{OH})_3$ upon contact with the water. Use of 0.2 M NaOH (as opposed to 1 M NaOH) was apparently sufficient for this transition.

2.4.4 5.6 M Na Simple Simulant Process Conditions

Approximately 11 to 12 L of 5.6 M Na simple simulant were processed sequentially through each of the ion exchange CST beds at three different flowrates, one flowrate per assembly. After simulant processing, 6 BVs of 0.1 M NaOH feed displacement and then 6 BVs of deionized water rinse were passed through the system, with one exception. The green column was accidentally pumped dry overnight while processing feed; in this case, the feed displacement and water rinse steps were abandoned. All processing was conducted at ambient temperature conditions, ranging from 18 to 22 °C. Test parameters, including process volumes, flowrates, and contact times, are summarized in Table 2.5 through Table 2.7 for each of the colored systems. The feed volume processed through the lag column is lower than that of the lead column because sample material collected from the lead column was not processed through the lag column.

Table 2.5. Experimental Conditions for the Red Column, 1.19 BV/h

Process Step	Solution	Total Volume			Flowrate		Time
		BV	AV	mL	BV/h	mL/min	h
<i>5.6 M Na Simple Simulant Test, 3/5/18 Start</i>							
Conditioning	0.2 M NaOH	5.77	1.21	57.7	3.04	0.506	1.90
Loading (lead)	Simulant	1112	--	11,124	1.19	0.198	935
Loading (lag)	Simulant	1075	--	10,750	1.19	0.198	935
Feed displacement	0.1 M NaOH	6.12	1.28	61.2	3.38	0.564	1.82
Water rinse	DI water	5.44	1.14	54.4	3.20	0.534	1.70

BV = bed volume is 10 mL as loaded in the column, see Section 2.4.2.

AV = apparatus volume (nominally 47.6 mL).

DI = deionized.

Table 2.6. Experimental Conditions for the Blue Column, 1.99 BV/h

Process Step	Solution	Total Volume			Flowrate		Time
		BV	AV	mL	BV/h	mL/min	h
<i>5.6 M Na Simple Simulant Test, Columns in Series, 3/5/18 Start</i>							
Conditioning	0.2 M NaOH	5.66	1.18	56.6	2.76	0.460	2.05
Loading (lead)	Simulant	1194	--	11,938	1.99	0.332	603
Loading (lag)	Simulant	1142	--	11,415	1.99	0.332	603
Feed displacement	0.1 M NaOH	5.93	1.23	59.3	3.00	0.499	1.98
Water rinse	DI water	5.98	1.24	59.8	3.02	0.503	1.98

BV = bed volume is 10 mL as loaded in the column, see Section 2.4.2.

AV = apparatus volume (nominally 48.1 mL).

DI = deionized.

Table 2.7. Experimental Conditions for the Green Column, 4.56 BV/h

Process Step	Solution	Total Volume			Flowrate		Time
		BV	AV	mL	BV/h	mL/min	h
<i>5.6 M Na Simple Simulant Test, Columns in Series, 4/2/18 Start</i>							
Conditioning	0.2 M NaOH	6.03	1.52	60.3	2.94	0.490	2.05
Loading (lead)	Simulant	1163	--	11,632	4.56	0.759	256
Loading (lag)	Simulant	1142	--	11,419	4.56	0.759	256
Feed displacement ^(a)	0.1 M NaOH	--	--	--	--	--	--
Water rinse ^(a)	DI water	--	--	--	--	--	--

(a) The column was pumped dry overnight while processing simulant feed. Feed displacement and water rinse steps were abandoned.

BV = bed volume is 10 mL as loaded in the column, see Section 2.4.2.

AV = apparatus volume (nominally 39.7 mL).

DI = deionized.

During the loading phase, nominal 10-mL samples were collected from the lead and lag columns at sample collection ports (Valves 2 and 3). The solution in the lag column remained static during the lead column sampling time of 20 to 50 min, depending on the flowrate. Samples were collected after the first

~10 BVs were processed and again at nominal 30- to 50-BV increments. Feed displacement and water rinse were collected in nominal 1-BV increments; each sample was submitted for GEA.

Cesium load performance was determined from the ^{137}Cs tracer concentration in the collected samples relative to the ^{137}Cs tracer in the feed. The collected samples were analyzed directly to determine the ^{137}Cs concentration using GEA. Cesium load breakthrough curves were generated based on the feed ^{137}Cs concentration (C_0) and the effluent Cs concentration (C) in terms of $\%C/C_0$.

With increased loading, the lead column appeared to become discolored. It was assumed that metals were either exchanging onto the CST or that solids were collecting at the top of the CST column. Figure 2.5 shows images of the Red lead and lag columns. Slight discoloration was visible at the top approximately 2 cm of the lead column. The presence of the clamp and accompanying shadows may make this observation difficult. This pattern was also observed for the Blue and Green columns.

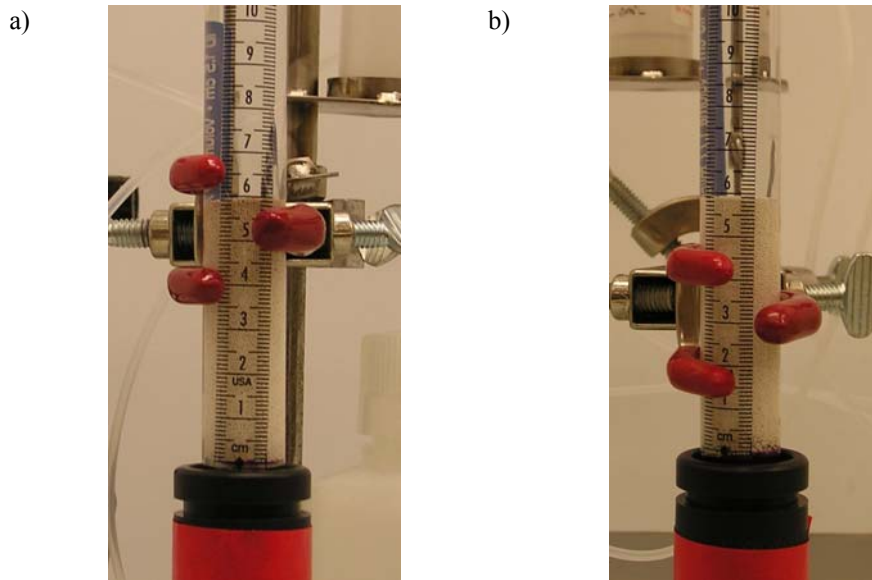


Figure 2.5. Red Columns a) Lead and b) Lag following Load Step Showing Slight Discoloration on Top of Lead Column

The last water rinse sample collected from the Blue column was measured for pH using ColorpHast pH paper (11 – 13 pH units, EM Science) for indication only. The fluid pH was ≥ 13 .

The Blue lead and lag columns were drained of fluid and submitted for axial gamma scan analysis to determine the Cs load profile over the axial distribution of the CST bed. The fluids drained from the lead and lag Blue columns following a settling period of about 24 hours are shown in Figure 2.6. Clearly, brown sediment was present in the Blue lead column drained fluid having the appearance of precipitated iron hydroxide. The samples were counted using GEA for information only because the sample geometry was slightly different from the calibrated 10 mL geometry. The lead column fluid resulted in $4.46\text{E-}03$ ^{137}Ci (approximately 0.84% C/C_0) and the lag column drained fluid resulted in $2.35\text{E-}3$ $\text{Ci } ^{137}\text{Cs}$ (approximately 0.44% C/C_0). Chemical analysis of this fluid/sediment was not conducted. The drained lead column CST bed reverted back to the typical white CST color.



Figure 2.6. Drained Fluids from the Blue Lead and Lag Columns Showing Sediment from Lead Column

The axial column GEA measurements were conducted using a St. Gobain BriLance-380 LaBr₃(Ce) detector (Model 38 S 38) coupled to a Canberra Osprey, digital MCA tube base. Detector parameters, data acquisition and data reduction were conducted on a Win7 PC running Canberra's Genie 2K gamma spectroscopy suite (V3.4). The detector was shielded on all sides by a minimum of 5 cm of lead. The face of the LaBr detector was approximately 0.5 cm from a lead collimator that was placed between the detector and the ion exchange column. The lead collimator was constructed from two, low-background lead, standard-dimension lead bricks (nominally 5 × 10 × 20 cm height, width, length). One of the bricks had a 1-mm-deep by 14-mm-wide channel machined down the center of the entire 20-cm length of the brick. The other brick was held tight against the collimator channel with four lag bolts. This final collimator assembly was 10 × 10 × 20 cm and weighed roughly 23 kg. The collimated path was 0.1 × 1.4 × 20 cm. Additional lead bricks were fashioned around the collimator and detector to prevent inadvertent radiation from streaming from the column, and the laboratory background. The ion exchange column was secured in a vertical linear mover that provided approximately 2.15 mm vertical travel for each full revolution of the threaded shaft screw. The outer edge of glass ion exchange column was approximately 2 cm from the collimator slit. Scanning was started with the CST bed below the collimator slit, and the threaded shaft screw turned clockwise to raise the resin bed into the "field of view" of the collimator and detector. The columns each had roughly 6 cm (60 mm) of packed CST. The lead column was scanned at 2.15-mm intervals (1 turn of threaded shaft screw). The lag column was scanned at 4.30-mm intervals (two turns of threaded shaft screw). Figure 2.7 shows an image of the entire system and an image of the lead column positioned next to the collimator.

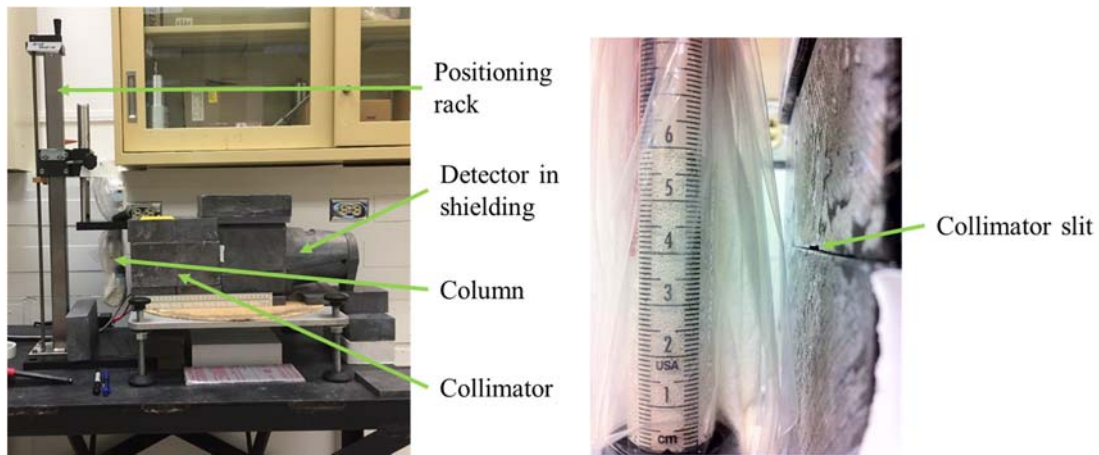


Figure 2.7. Axial Gamma Scan Analysis System

2.5 Sample Analysis

Samples were analyzed directly (no preparation) for ^{137}Cs by GEA. No dilutions or other preparations were required. All analyses were conducted by the Analytical Support Operations (ASO) according to standard operating procedures, the ASO Quality Assurance Plan, and the ASR.

3.0 Batch Contact Results

This section discusses the batch contact results for the 5.6 M Na simulant with CST.

3.1 5.6 M Na Simulant Batch Contact Results

The K_d values versus Cs concentrations are provided in Table 3.1 and plotted in Figure 3.1 on a linear-log scale. Note that the primary samples were contacted for 24 hours and the duplicates were contacted for 45 hours. The K_d vs. the log of the Cs equilibrium concentration was curve-fitted to a second order polynomial equation to calculate the K_d at the feed concentration of 8.0 $\mu\text{g/mL}$: 690 mL/g (24-hour contact time) and 770 mL/g (45-hour contact time). The theoretical 50% Cs breakthrough on the ion exchange column (λ) can be predicted from the product of the K_d value and the ion exchanger bed density (ρ_b) (see Eq. (3.1)). The CST bed density is the dry CST mass divided by the volume in the column. For this assessment, the CST bed density was 1.0 g/mL. The theoretical 50% breakthrough (λ) for 5.6 M simple simulant with 8.0 $\mu\text{g/mL}$ Cs is 770 BVs based on the 45-hour contact time.

$$K_d \times \rho_b = \lambda \quad (3.1)$$

Table 3.1. Equilibrium Results for Batch Contact Samples in 5.6 M Na Simple Simulant

Sample ID	Initial [Cs], $\mu\text{g/mL}$	Final [Cs], $\mu\text{g/mL}$	K_d , mL/g	Equilibrium Cs in CST, mg Cs/g
TI035-S1-BC	7.97	1.64	730	1.20
TI035-S2-BC	39.1	8.77	676	5.82
TI035-S3-BC	199	53.1	530	27.4
TI035-S4-BC	930	591	114	65.4
TI035-S5-BC	6152	5940	6.9	40.9
TI035-S1-BC-d	7.97	1.55	785	1.21
TI035-S2-BC-d	39.1	7.21	813	5.86
TI035-S3-BC-d	199	49.9	558	28.0
TI035-S4-BC-d	930	558	120	66.7
TI035-S5-BC-d	6152	5872	8.8	51.7

Note that the 5.6 M Na simple simulant also contains 0.122 M K and 1.41 M free hydroxide.

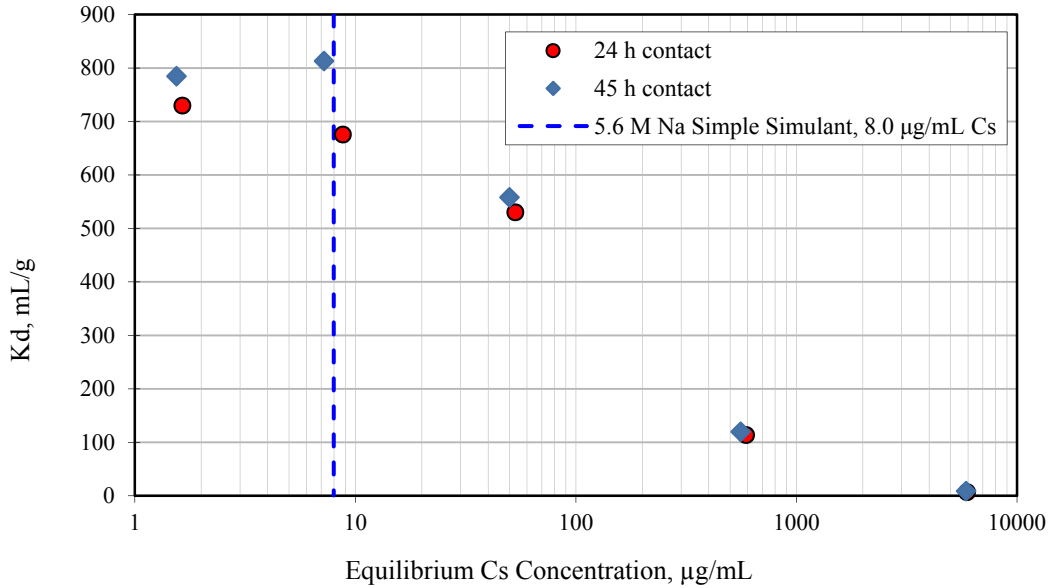


Figure 3.1. Equilibrium Cs K_d Curve for 5.6 M Na Simple Simulant with CST

Figure 3.2 compares the K_d values obtained with this test batch of CST in 5.6 M Na simple simulant with those reported by Brown et al. (1996), CST batch 0739-38B, in two other materials (actual tank waste and 5 M Na simulant tank waste). The double-shell slurry feed (DSSF) tank waste was formulated from a blend of tank wastes (70% from AW-101, 20% from AP-106, and 10% from AP-102) and contained 5.0 M Na, 0.44 M K, and 2.0 M free hydroxide. The simulant DSSF tank waste was similarly constructed to contain 5 M Na, 0.475 M K, and 2.17 M free hydroxide. The 5.6 M Na simple simulant, consisting of 0.122 M K and 1.41 M free hydroxide, results agreed closely with the results from the DSSF tank waste. The DSSF simulant in contrast had much higher K_d values at low Cs concentrations. Brown et al. (1996) could not determine the reason the actual and simulant tank waste results diverged.

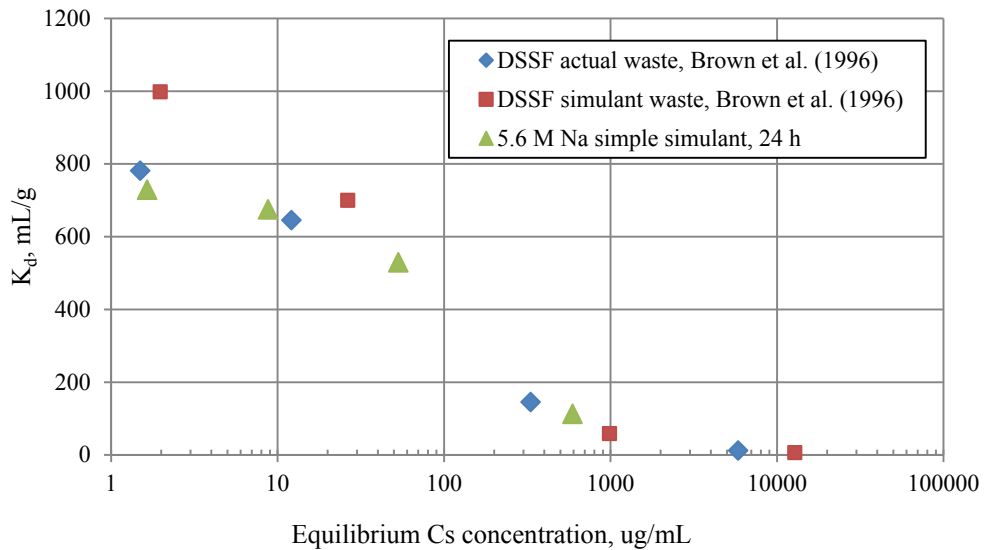


Figure 3.2. Comparison of Current Test (24-hour Contact Time) with Brown et al. (1996) Data

Figure 3.3 provides the isotherm for the 5.6 M Na simple simulant batch contact test samples (excluding the high Cs concentration sample initial concentration of 6152 µg/mL). In this case, the equilibrium Cs concentration is expressed in terms of mg/mL (as opposed to µg/mL in Figure 3.1). The isotherm was fitted to the Langmuir adsorption equation according to Eq. (3.2). The expected Cs loading onto the resin at a given Cs concentration can be determined from the isotherm.

$$\frac{837 \times [Cs]}{(10.9 \times [Cs]+1)} = C_{SIX} \quad (3.2)$$

where [Cs] = equilibrium Cs concentration in solution, mg Cs per mL solution

C_{SIX} = equilibrium Cs loading on the CST, mg Cs per g CST

At the equilibrium Cs concentration of 8.0 µg/mL (0.0080 mg/mL), the equilibrium Cs loading corresponds to 6.16 mg Cs per g dry CST.

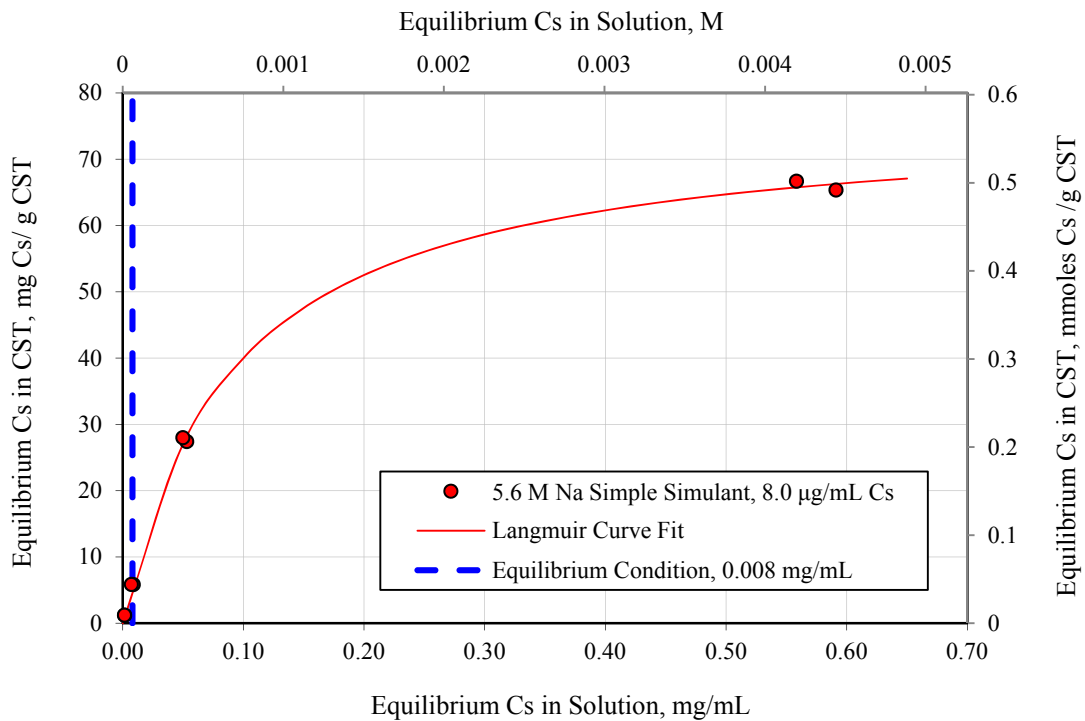


Figure 3.3. Isotherm for the 5.6 M Na Simple Simulant with CST

4.0 Column Test Results

The Cs load behavior was evaluated at three different flowrates with the 5.6 M Na simple simulant. This section discusses the load, feed displacement, water rinse, and Cs mass balance results for the three tests. Raw data are provided in Appendix A.

4.1 Cs Load, Feed Displacement, and Water Rinse Results

The Red columns processed feed at 1.19 BV/h. Figure 4.1a shows the Cs load profiles for the lead and lag columns on a linear-linear plot. The x-axis shows the BVs processed and the y-axis shows the effluent Cs concentration (C) relative to the feed concentration (C_0) in terms of $\%C/C_0$. In this graphing format, the Cs breakthrough from the lead column appears to start at ~220 BVs and continues to 1110 BVs (a range of 890 BVs). The lead column 50% breakthrough was at ~800 BVs. The lag column Cs breakthrough appears to have started at ~750 BVs. The breakthrough profile in relation to the contract limit is not discernable on this linear/linear scale. Figure 4.1b shows the same Cs load data provided in Figure 4.1a on a probability-linear scale plot. Under ideal conditions, the Cs load profile will appear linear on the probability plot, allowing for backward and forward extrapolations. Further, the probability plot shows much more detail for the performances of the lead and lag columns at low and high $\%C/C_0$ values and especially in relation to the contract limit. The contract limit was assigned 0.114 $\%C/C_0$.¹

Figure 4.1b shows that Cs breakthrough from the lead column starts after processing 52 BVs and the contract limit is reached after processing just 162 BVs. The effluent from the lag column breakthrough starts at ~329 BVs and reaches the contract limit at ~590 BVs. It is also interesting to note that the lead column Cs breakthrough profile demonstrates curvature whereas the lag column Cs breakthrough appears nearly linear. The reason for these two different curve shapes is not clear.

Figure 4.2 and Figure 4.3 show the Cs breakthrough profiles for the Blue (1.99 BV/h) and Green (4.56 BV/h) columns using both y-axis scales. In all cases, the Cs load curves were not smooth—there were regions of erratic loading such as exhibited by the Blue lead column at 715 to 940 BVs, where two plateau steps were observed. The Green lead column exhibited a similar aberration between 980 and 1123 BVs. The reason for these aberrations is not clear. In contrast, breakthrough profiles measured with spherical resorcinol formaldehyde resin were smooth, allowing for simple interpolation between data points and backward and forward extrapolations (Fiskum et al. 2018).

¹ The contract limit was based on AP-107 tank waste with 5.61 M Na and 156.5 $\mu\text{Ci/mL}$ ^{137}Cs and a maximum loading of $3.18\text{E-}5$ Ci ^{137}Cs /mole Na in the glass (from the ICD-30 Waste Acceptance Criterion).

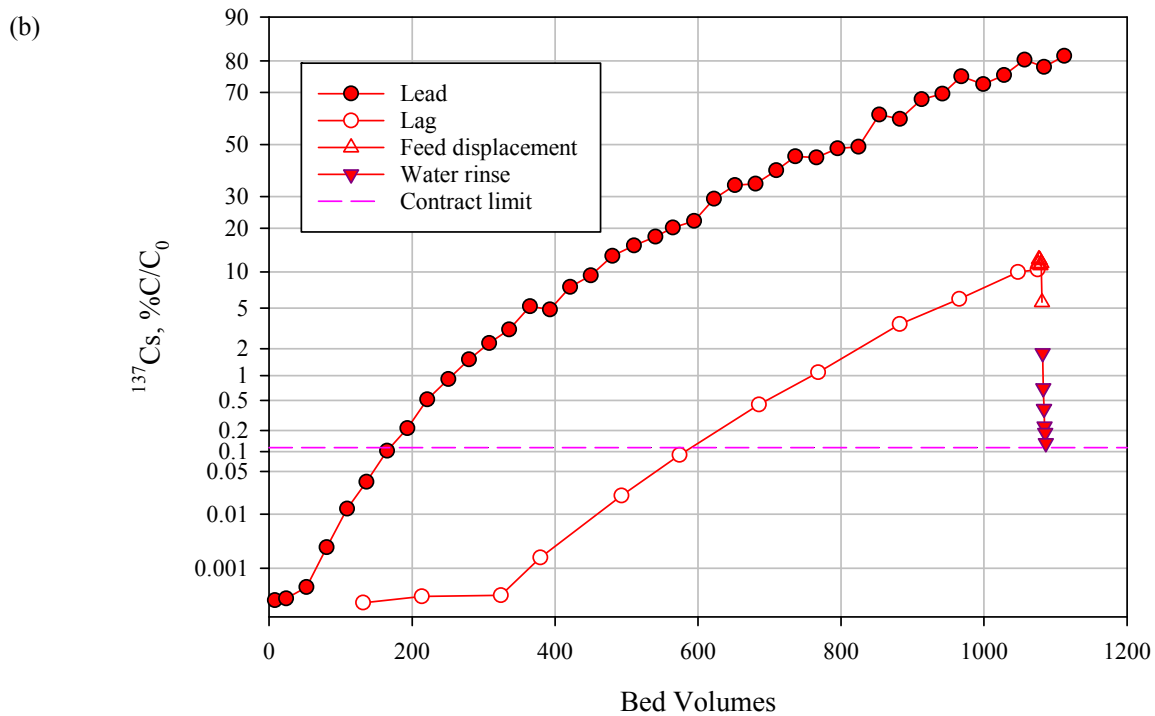
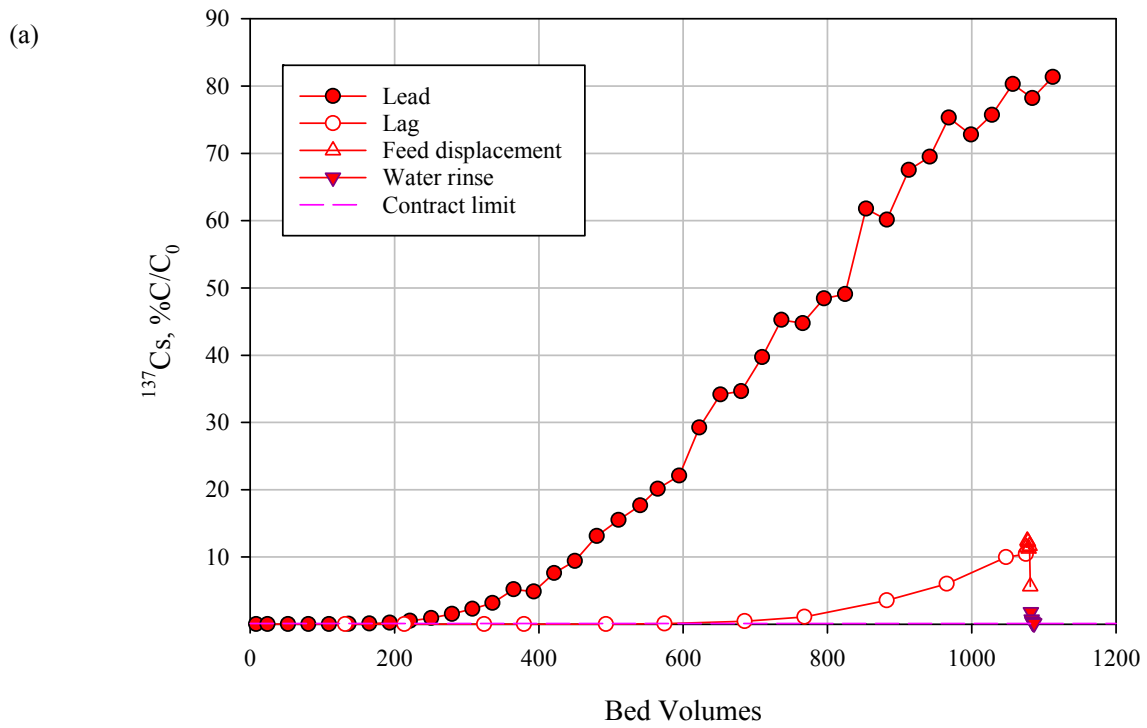


Figure 4.1. Lead and Lag Column Cs Load Profiles of 5.6 M Na Simple Simulant with 8.0 $\mu\text{g/mL}$ Cs at 1.19 BV/h (a) Linear-Linear Plot, (b) Probability-Linear Plot

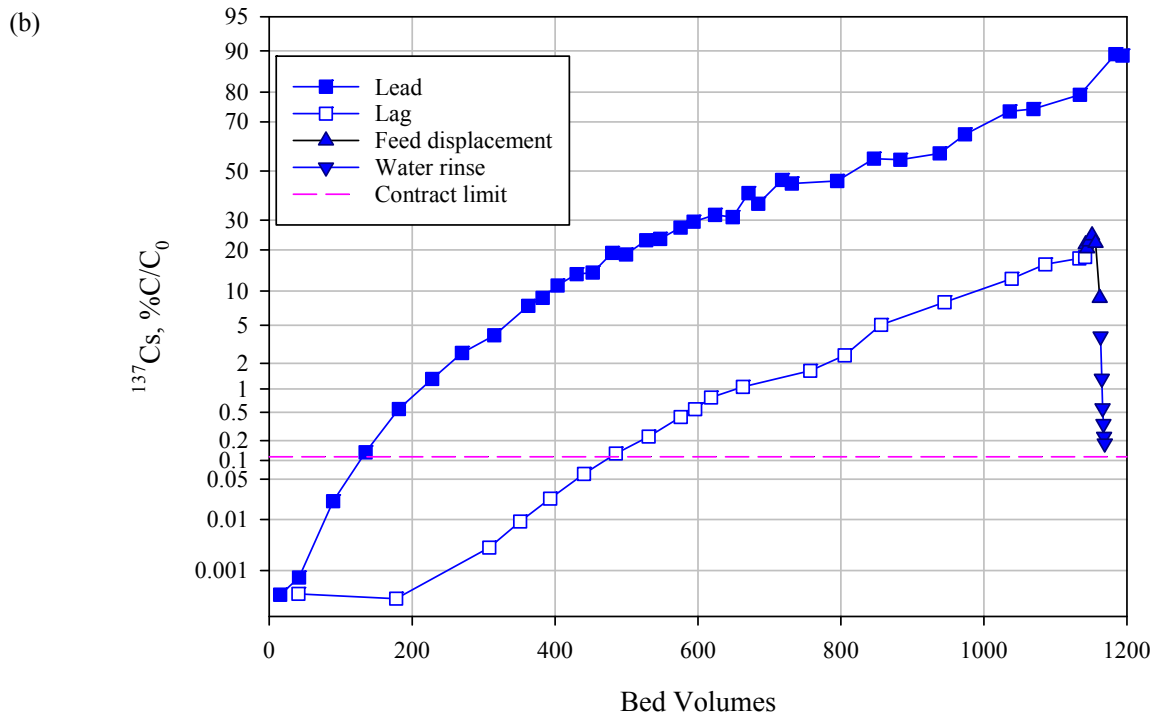
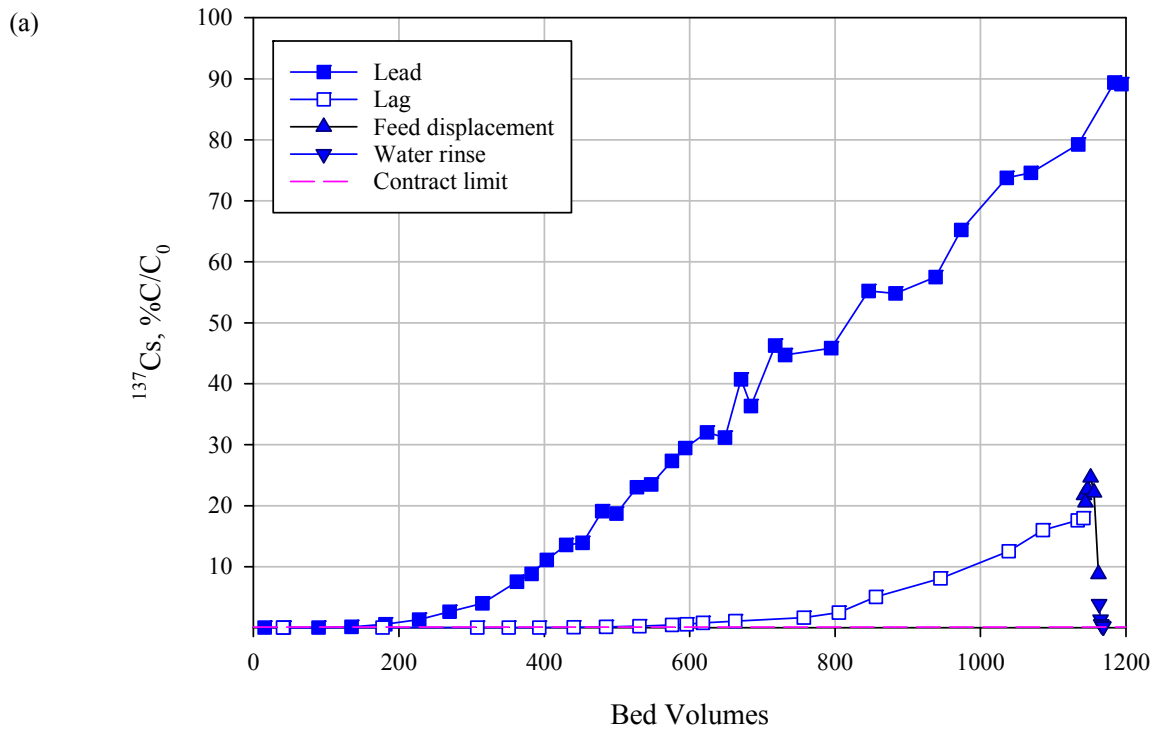


Figure 4.2. Lead and Lag Column Cs Load Profiles of 5.6 M Na Simple Simulant with 8.0 $\mu\text{g/mL}$ Cs at 1.99 BV/h (a) Linear-Linear Plot, (b) Probability-Linear Plot

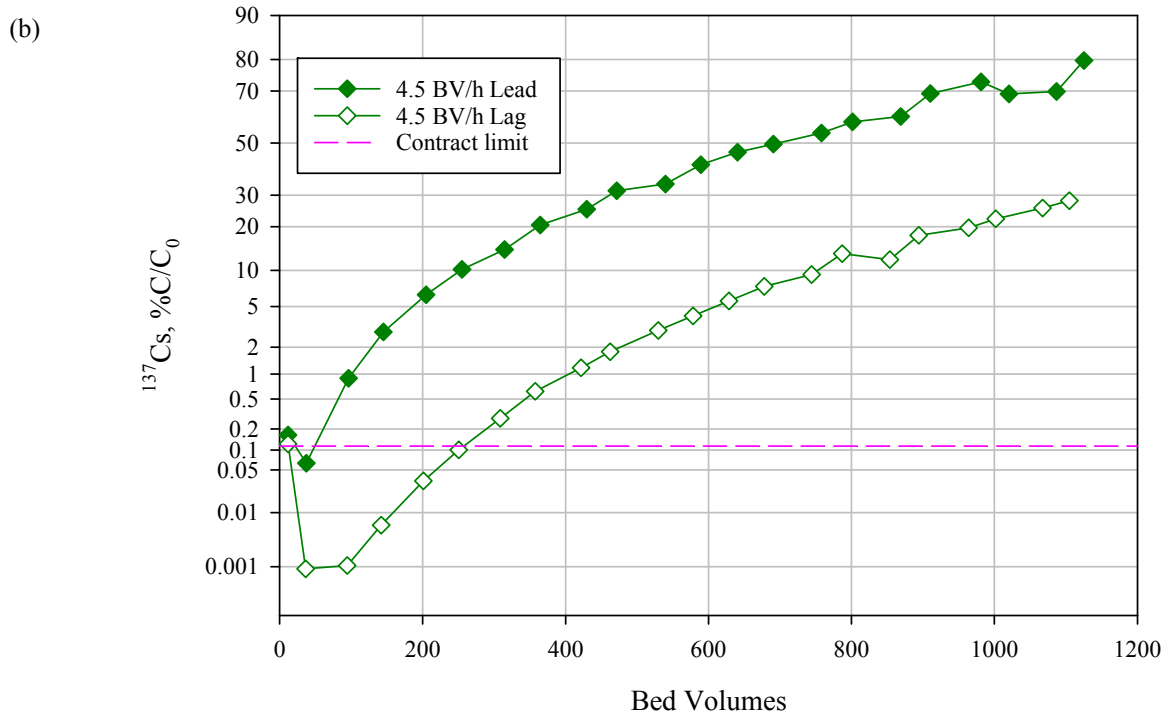
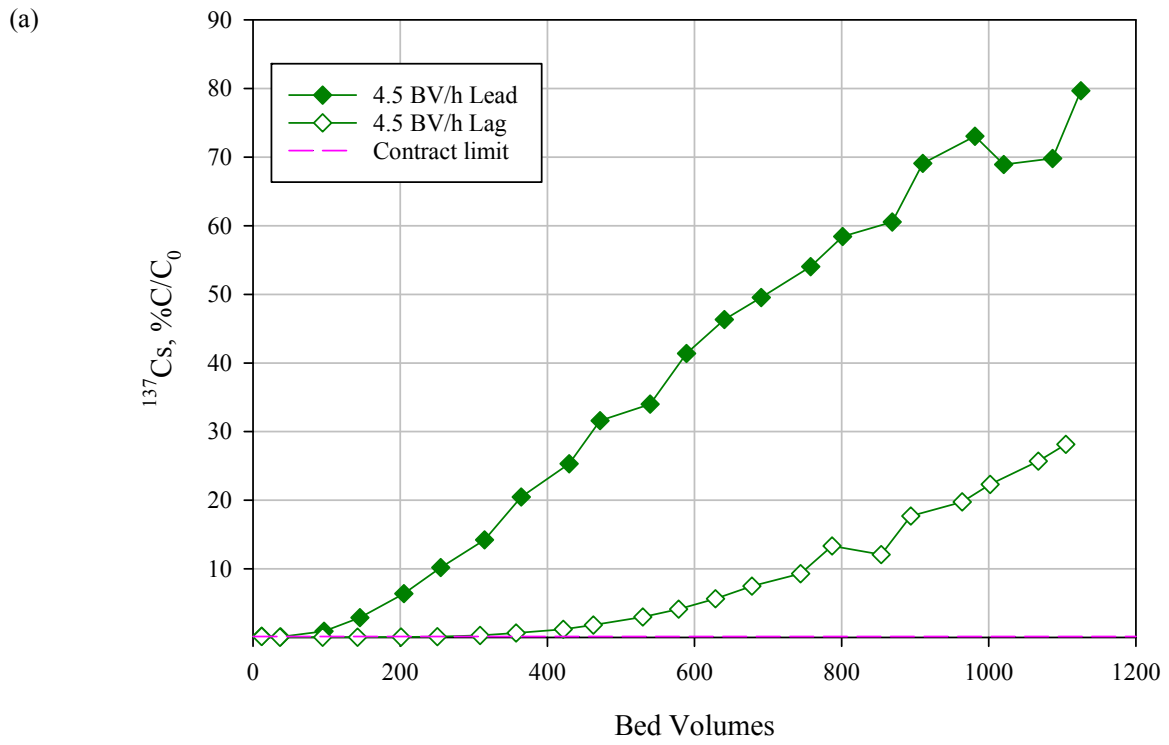


Figure 4.3. Lead and Lag Column Cs Load Profiles of 5.6 M Na Simple Simulant with 8.0 $\mu\text{g/mL}$ Cs at 4.56 BV/h (a) Linear-Linear Plot, (b) Probability-Linear Plot

The feed displacement following 5.6 M Na simple simulant feed was shown to simply extend the lag column Cs breakthrough profile, as would be expected because the feed displacement pushes out the 5.6 M Na simple simulant feed existing in the system. Of greater interest is the effect of the water rinse that followed the feed displacement. The effluent collection of the water rinse would be mostly composed of the feed displacement solution (0.1 M NaOH). As the contact solution changed from 5.6 M Na simple simulant to 0.1 M NaOH, Cs leakage from the lag column noticeably dropped off. This indicates that the Cs remained adsorbed into the CST while the ionic strength of the solution decreased.

4.2 Column Gamma Scan

The lead and lag Blue columns were scanned top to bottom by GEA to assess the overall nature of the Cs loading onto the CST. Use of the 0.1 mm high \times 14 mm wide \times 20 cm long collimator provided the means to differentiate activity at a specific point from activity at other points in the column. Figure 4.4 shows the gamma scan results. The y-axis shows the CST bed height position where “0” marks the top of the bed and 60 marks the bottom of the bed. The x-axis shows the gamma count rate in terms of counts per second. The analysis does not represent a calibrated geometry from which actual ^{137}Cs concentrations are measured; it is simply intended to show relative ^{137}Cs activity across the column.

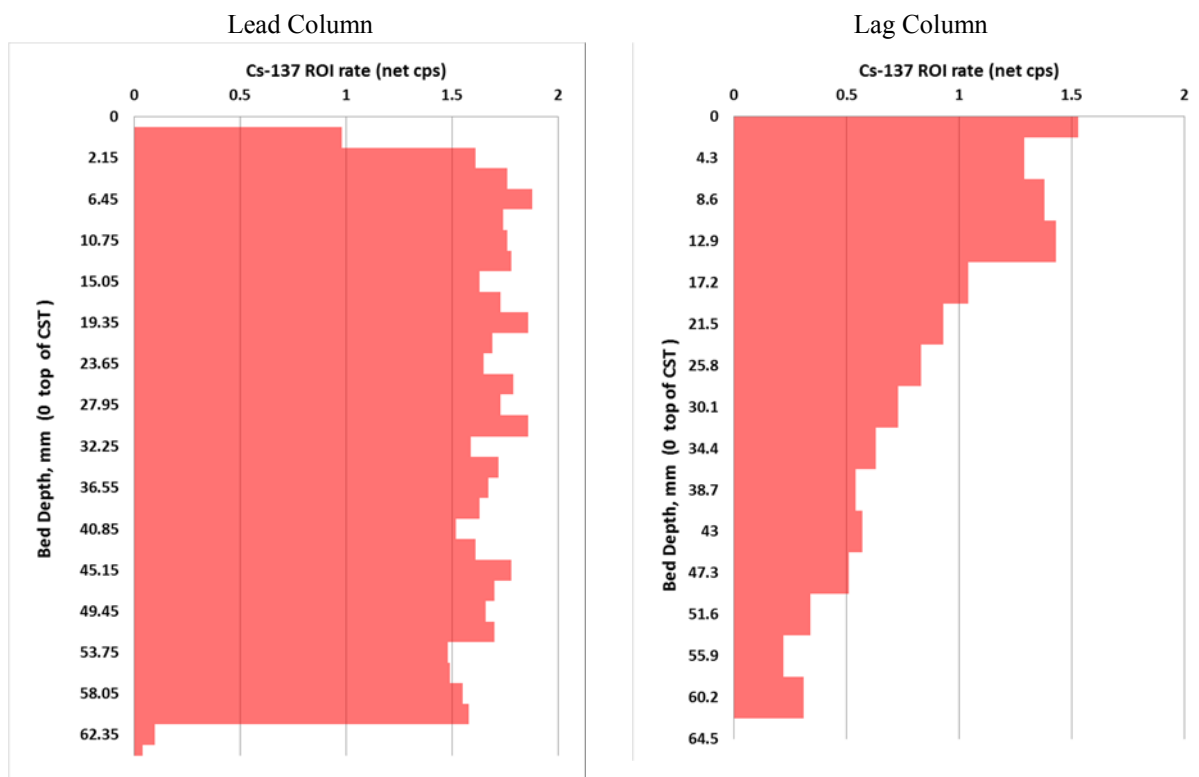


Figure 4.4. Lead and Lag Blue Column System Gamma Scans Showing Relative ^{137}Cs Activity

The nearly 0 counts per second measured at 62.3 and 64.5 mm on the lead column indicated that minimal shine interference from adjacent points on the CST column occurred. Thus, the count rate measured for each discrete location is not affected by neighboring regions. This image indicates that the lead column was uniformly loaded (top to bottom) with Cs. The lag column, in contrast, shows Cs primarily at the top

of the bed with tapering toward the bottom of the bed. These results met expectations for how Cs loads onto the CST bed.

4.3 Cesium Activity Balance from Ion Exchange Processing

Table 4.1 through Table 4.3 summarize the ^{137}Cs fractionation between the effluents (collected in multiple collection bottles), samples collected during the load processing, feed displacement, water rinse, and Cs loaded onto the lead and lag columns. The total Cs fractionation is the same as the ^{137}Cs fractionation. The 8.0 $\mu\text{g/mL}$ Cs in the feed corresponds to $\sim 0.054 \mu\text{Ci/mL}$ ^{137}Cs tracer in the feed. The total of amount of ^{137}Cs varied slightly from one test to the next based primarily on the total volume processed. Excellent activity balance (100% accounted for) was obtained for all tests. The quantities of Cs loaded onto the lead and lag columns were determined by subtracting the integrated area under the associated load curve from the total quantity fed to the associated column. About 63% to 73% Cs loaded onto the lead column and 30% to 25% loaded onto the lag column. Sample and effluent collection amounted to 3% to 8% of the input Cs.

Table 4.1. ^{137}Cs Activity Balance for the Red Column Test

Input	$\mu\text{Ci } ^{137}\text{Cs}$	%
Feed Sample	607	100
Output	$\mu\text{Ci } ^{137}\text{Cs}$	%
Effluent-1 (0-365 BVs)	<1.5E-3	<2.5E-4
Effluent-2 (366-710 BVs)	0.138	0.0227
Effluent-3 (711-913 BVs)	2.53	0.416
Effluent-4 (914-1112 BVs)	7.73	1.27
Load samples	6.17	1.02
Feed displacement	0.356	0.0587
Water rinse	0.0168	2.76E-03
Lead column Cs loading	443	73.0
Lag column Cs loading	149	24.6
Output sum	609	100.3%
Tracer: 0.0543 $\mu\text{Ci } ^{137}\text{C/mL}$ simulant.		
6.81E-3 $\mu\text{Ci } ^{137}\text{C}/\mu\text{g Cs}$		

Table 4.2. ^{137}Cs Activity Balance for the Blue Column Test

Input	$\mu\text{Ci } ^{137}\text{Cs}$	%
Feed Sample	632	100
Output	$\mu\text{Ci } ^{137}\text{Cs}$	%
Effluent-1 (0-362 BVs)	2.96E-03	4.68E-04
Effluent-2 (363-731 BVs)	0.838	0.133
Effluent-3 (732-938 BVs)	3.863	0.611
Effluent-4 (939-1134 BVs)	9.5	1.50
Effluent-5 (1135-1194 BVs)	5.2	0.816
Load samples	6.1	0.967
Feed displacement	0.630	0.100
Water rinse	0.035	5.46E-03
Lead column Cs loading	417	66.0
Lag column Cs loading	190	30.1
Output sum	633	100.2%
Tracer: 0.0530 $\mu\text{Ci } ^{137}\text{C}/\text{mL}$ simulant. 6.64E-3 $\mu\text{Ci } ^{137}\text{C}/\mu\text{g Cs}$		

Table 4.3. ^{137}Cs Activity Balance for the Green Column Test

Input	$\mu\text{Ci } ^{137}\text{Cs}$	%
Feed Sample	647	100
Output	$\mu\text{Ci } ^{137}\text{Cs}$	%
Effluent-1 (0-364 BVs)	0.295	0.05
Effluent-2 (365-758 BVs)	6.81	1.05
Effluent-3 (759-1125 BVs)	41.7	6.44
Load samples	5.35	0.827
Water rinse	NA	NA
Feed displacement	NA	NA
Lead column Cs loading	414	64.0
Lag column Cs loading	179	27.6
Output sum	647	100.0%
Tracer: 0.0557 $\mu\text{Ci } ^{137}\text{C}/\text{mL}$ simulant. 6.99E-3 $\mu\text{Ci } ^{137}\text{C}/\mu\text{g Cs}$		

The Cs load capacity was calculated from the total Cs loaded onto the lead column, which was assumed to be fully saturated under these load conditions, and the dry CST mass loaded into the lead column according to Eq. (4.1).

$$\frac{A_{Cs} \times CF}{M} = C \quad (4.1)$$

- where A_{Cs} = activity of ^{137}Cs , μCi on the lead column
 CF = conversion factor, $\mu\text{g Cs}/\mu\text{Ci } ^{137}\text{Cs}$, specific to the Cs and ^{137}Cs spike conditions of each test
 M = mass of dry CST (9.8289 g)
 C = capacity, mg Cs/g CST

Table 4.4 summarizes the CST capacities for each test. The decrease in Cs capacity with increasing flowrate is attributed to the kinetic limitations of the Cs exchange onto CST. Batch contact testing resulted in a capacity 6.16 mg Cs/g CST at 8.0 $\mu\text{g/mL}$ Cs equilibrium condition, approximately 3% lower than the column average result. The 3% difference cannot be excluded from overall experimental uncertainties.

Table 4.4. Cs Capacity in CST

Column Test	Flowrate, BV/h	Capacity, mg Cs/g CST	Capacity, mmoles Cs/g CST
Red	1.19	6.61	0.0498
Blue	1.99	6.38	0.0480
Green	4.56	6.03	0.0454

4.4 Measured and Predicted 50% Cs Breakthrough

Figure 4.5 shows the lead column Cs load profile for each test. Clearly, the Green column test reached the 50% breakthrough (~690 BVs) earlier than the Red and Blue column tests (~800 BVs).

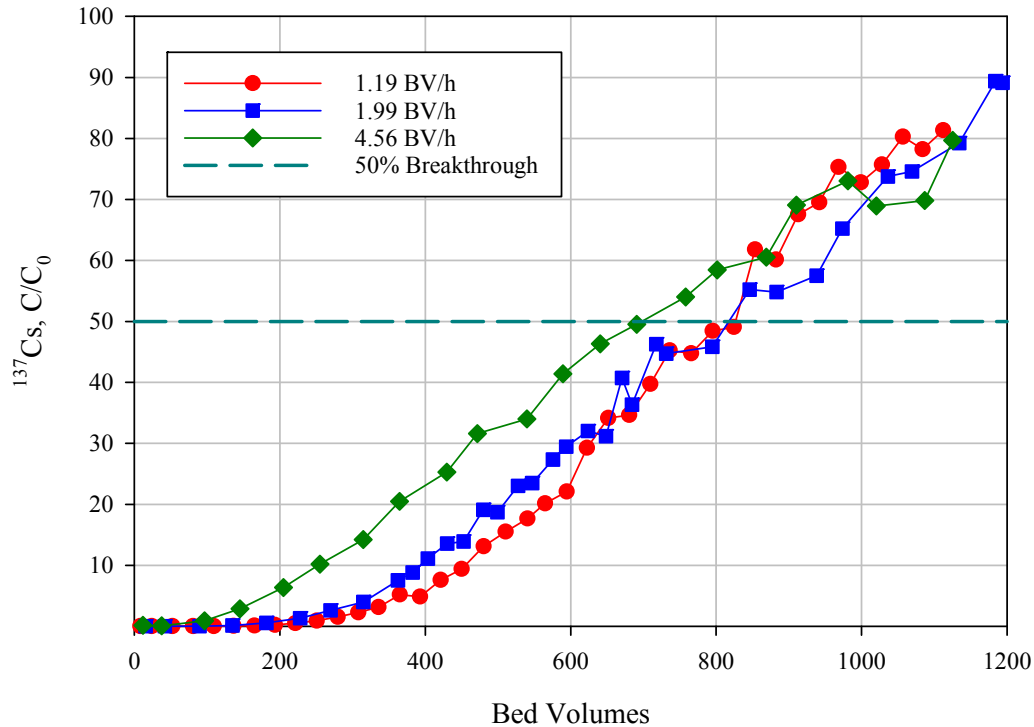


Figure 4.5. Lead Column Comparison

The K_d determination from the batch contact test is typically used to estimate the 50% breakthrough according to Eq. (4.2), where ρ_b is the CST bed density (in this case, 1.00 g/mL) and λ is the BVs at 50% C_s breakthrough.

$$K_d \times \rho_b = \lambda \quad (4.2)$$

The λ value (predicted 50% C/C_0 breakthrough) of 770 BVs determined from batch contacts closely matched that observed for the Red and Blue columns (4% difference). The batch contact testing was a good indicator of column performance.

4.5 Contract Limit

Figure 4.6 plots the three lag column C_s load profiles. Clearly, inferior performance was realized at the fast flowrate of 4.56 BV/h, where contract limit was reached after processing ~250 BVs of feed. The Blue column system processed 475 BVs to contract limit and the Red column system processed 590 BVs to contract limit. Thus, more feed can be processed in the ion exchanger by decreasing flowrate and allowing for the kinetically slow C_s particle diffusion. Decreasing flowrate of course decreases throughput rate.

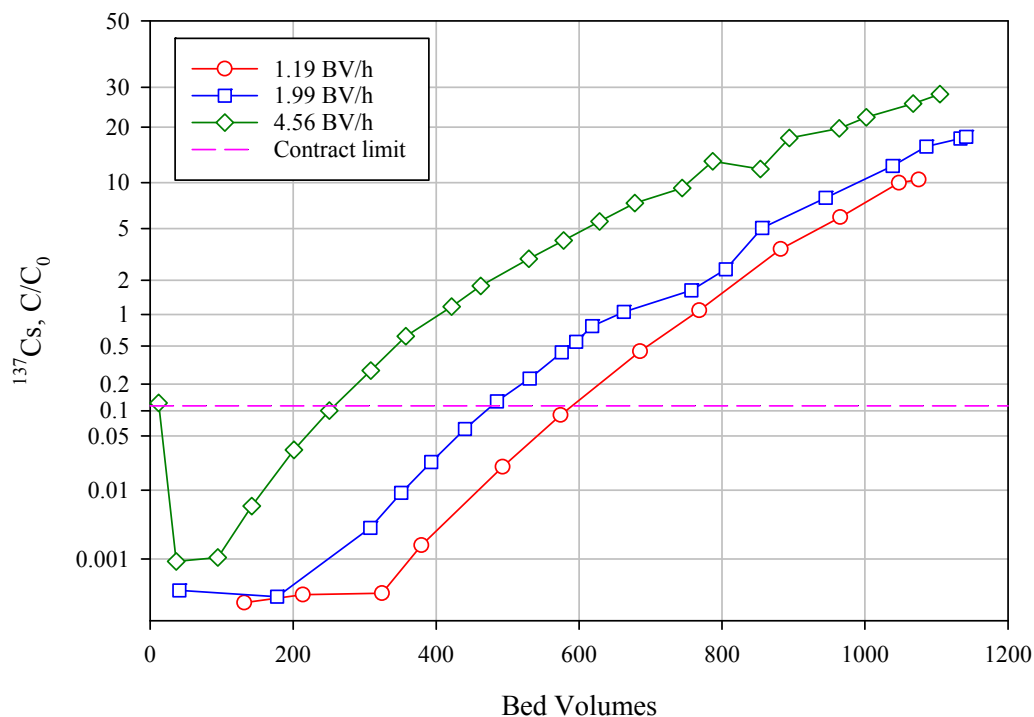


Figure 4.6. Comparison of Lag Column Performance

The effect of flowrate was further examined by looking at the test lead columns individually and the combined lead/lag column (as a combined system). For the latter case, the lead/lag column volumes were combined (20 mL total). This in effect halved the flowrate or doubled the residence time; for example, a 1.19-BV/h flowrate in a 10-mL CST bed would be halved to 0.60 BV/h in a 20-mL CST BV system. Table 4.5 shows the column systems, flowrates, and the BVs processed to reach the contract limit. Figure 4.7 shows the relationship of the processed volume as a function of flowrate before reaching the contract limit. In this case, the data were fit to a logarithmic curve. (A power curve fit also matches this data set well.) The curve was backward extrapolated to show that 400 system volumes *might* be processed before reaching contract limit if the flowrate was reduced to ~0.22 BV/h—however, this flowrate is beyond the test range and would need to be confirmed.

Table 4.5. Bed Volumes Processed to Reach Contract Limit

Test	Flowrate, SV/h	Contract Limit, BV
Red lead column	1.19	162
Blue lead column	1.99	129
Green lead column	4.56	48
Red 2-column system	0.60	294
Blue 2-column system	1.00	240
Green 2-column system	2.28	120

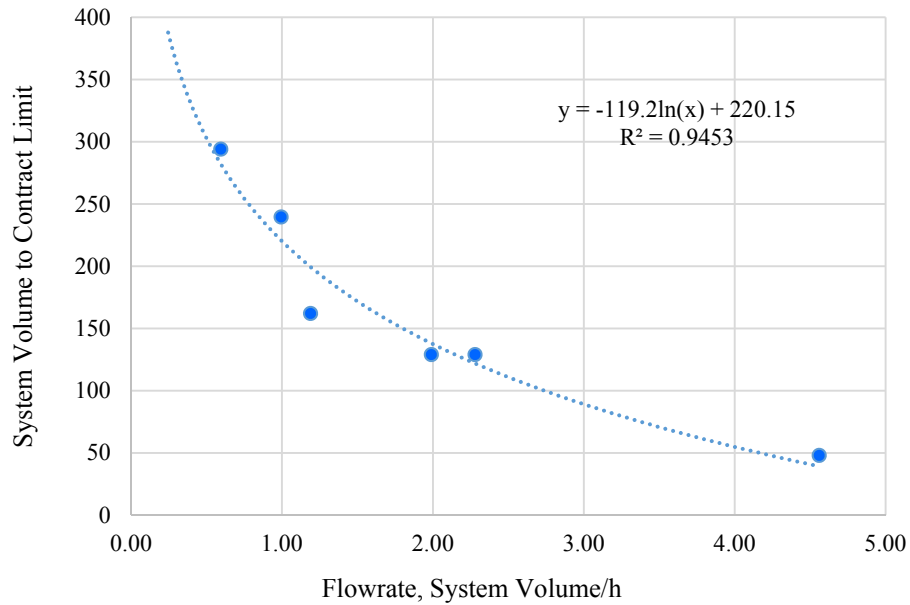


Figure 4.7. Volume Processed to Reach Contract Limit vs. Flowrate

The effect of flowrate on the Cs exchange into CST was further evaluated by comparing the Blue lead column at 1.99 BV/h to the Green two-column system at 2.28 BV/h. Although these flowrates are slightly different, the feed solution residence time in the CST bed is similar enough to compare the Cs breakthrough profiles. The linear flow velocities are 11.9 cm/h and 27.4 cm/h, for the Blue and Green systems, respectively. Figure 4.8 shows the Cs load profiles for these two systems. They are virtually identical from 0 to 550 BVs, indicating that the residence time, not the flow velocity, affects Cs exchange into the CST. Therefore, the Cs exchange rate is shown to not be affected by the linear flow velocity.

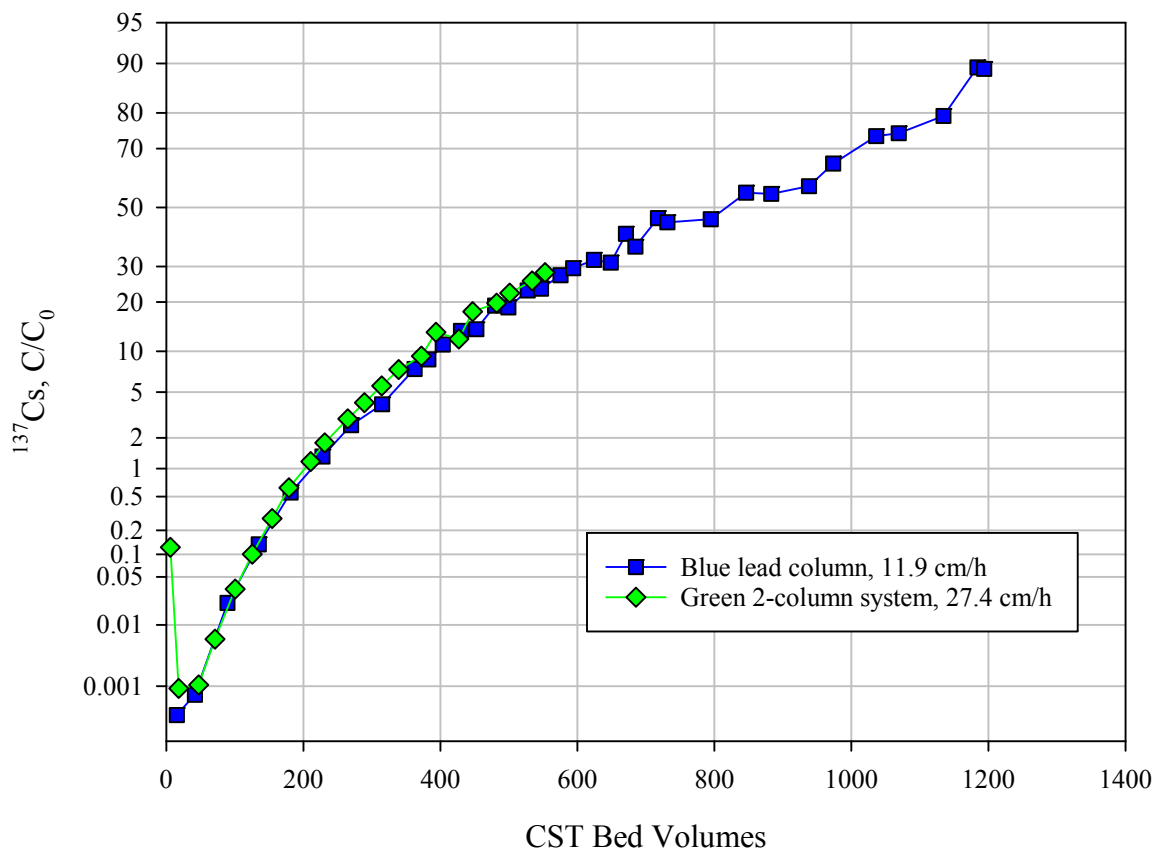


Figure 4.8. Cs Load Profiles at Two Different Linear Velocities and Nearly Constant Residence Time

4.6 Transition Zone

The transition (or exchange) zone is defined as the volume processed from the onset of Cs breakthrough to the full saturation of the ion exchanger where the effluent Cs concentration equals the influent Cs concentration. The 50% breakthrough point is the inflection point around which the transition zone pivots. In the current study, none of the tests reached full saturation of the lead column and the Blue and Red curves through the 50% breakthrough point were not uniform (estimated at 800 BVs, see Figure 4.5). Comparative transition zone characteristics between these tests were evaluated by looking at the limited range of 20% to 80% Cs breakthrough. The upper range of 80% was met for all tests; the lower range of 20% provided a symmetric basis at the low end. Table 4.6 shows the identified 20% and 80% Cs breakthrough points and the calculated transition zone (20% to 80% range). Within the flowrate range tested here, it is evident that slowing flowrate sharpens the transition zone. These observations are consistent with particle diffusion limited Cs exchange.

Table 4.6. Flowrate Effect on the Transition Zone

Test	Flowrate, BV/h	20% Cs Breakthrough, BVs	80% Cs Breakthrough, BVs	Transition Zone (20-80% Cs Breakthrough), BVs
Red lead column	1.19	565	1052	490
Blue lead column	1.99	490	1130	640
Green lead column	4.56	360	1125	765

The differences in Cs breakthrough (and thus transition zone) can be traced to ion exchange dynamics. In general, there are three steps to the absorption of material on ion exchange media (Harland 1994):

1. Transfer of the cesium from the bulk solution to the surface of the CST bead through the mass transfer layer (film diffusion)
2. Diffusion of the cesium within the CST bead from the surface to the ion exchange site (particle/pore diffusion)
3. Exchange of the cesium atom for a sodium atom at the ion exchange site (chemical reaction/ion exchange)

From Figure 4.8 it can be seen that film diffusion was not a factor in the Cs exchange rate—that is, increasing flow velocity did not change the Cs load profile. The exchange rate onto powdered CST from early production lots was shown to be rapid (Brown et al. 1996). In the powdered form, much more surface area is available for exchange relative to the surface area of the engineered form. The rate limiting step for Cs exchange into the CST is thus diffusion through the CST bead. Therefore, extending the tank waste residence time (equilibrium time) leads to greater utilization of the CST for cesium separation.

5.0 Conclusions and Recommendations

Both objectives for CST testing were met: 1) conduct simulant testing to evaluate Cs load curves as a function of flowrates on small column CST beds, and 2) conduct batch contact testing with CST to determine the 5.6 M Na simple simulant Cs K_d factor and load capacity.

5.1 Physical Properties

Several key physical properties of the tested production lot were measured.

- The material had a D10 of 419 microns, D50 of 573 microns, and D90 of 779 microns, consistent with a 20x40 mesh sieve cut from the manufacturer.
- The settled bed density was 1.00 g dry CST per milliliter of wetted CST volume.
- Bed void volume was 65.6%.
- The CST was generally round with rough surfaces and in some cases fracture lines. It was easily friable.
- The CST consisted of O, Ti, Zr, Nb, Na, and Si.

5.2 Batch Contact Testing

The batch contact testing was shown to predict elements of the column performance well.

- The measured K_d of 770 mL/g at the Cs equilibrium condition of 8.0 $\mu\text{g/mL}$, corresponding to a predicted 50% Cs breakthrough of 770 BVs, matched the column test results within ~3%.
- The Cs load capacity at 8.0 $\mu\text{g/mL}$ equilibrium condition of 6.16 mg Cs/g dry CST matched the column test results within ~7%.

However, batch contact testing does not relate to the slope of the Cs load curve, how the slope relates to flowrate, and thus cannot predict the contract limit breakthrough in terms of BVs.

5.3 Column Testing

Table 5.1 summarizes relevant Cs loading characteristics for the three different flowrates tested in the lead/lag column format.

Table 5.1. Column Performance Summary with 5.6 M Na Simple Simulant

Flowrate, BV/h	50% Cs Breakthrough, BV	Cs Loading Capacity, mg/g	Lag Column Contract Limit ^(a) , BV
1.19	800	6.61	590
1.99	800	6.38	475
4.56	690	6.03	260

(a) The contract limit is defined to be $0.114 C/C_0$, congruent with tank waste at 5.6 M Na and $156 \mu\text{Ci/mL } ^{137}\text{Cs}$. This corresponds to a decontamination factor of 878.

- Column performance indicated that Cs exchange was particle diffusion limited, not film diffusion limited. Large-scale tests would be needed to extrapolate this assertion to plant scale.
- As the flowrate increases, the BVs processed to reach the contract limit decreases with a negative logarithmic function. Extrapolation beyond the lower limit of the tested range indicated that a flowrate of ~ 0.4 BV/h would be required to approach the 800-BV capacity in the lead column while not passing the contract limit from the lag column.
- LAWPS would need to implement changes to achieve the plant objective of processing 1025 BVs of tank waste and achieve product at or below the contract limit. Changes could include slowing flowrate (from planned 1.4 BV/h), increasing the column length, or adding a third column.

5.4 Recommendations for Future Testing

Recommendations for future testing include the following:

1. Parametric batch contact testing to elucidate the effects of competing anion and cation concentrations in ranges relevant to Hanford tank waste on Cs ion exchange capacity.
2. Batch contact kinetic studies test to confirm the time required to obtain equilibrium Cs concentration in the new CST formulation. This information would be used to support follow-on batch contact studies.
3. Scale up testing to establish the relationship of small column tests to pilot scale and full scale processes.

6.0 References

ASTM E11, *Standard Specification for Woven Wire Test Sieve Cloth and Test Sieves*. 2017. ASTM International, West Conshohocken, Pennsylvania.

Brown, GN, LA Bray, CD Carlson, KJ Carson, JR DesChane, RJ Elovich, FV Hoopes, DE Kurath, LL Nenninger, and PK Tanaka. 1996. *Comparison of Organic and Inorganic Ion Exchangers for Removal of Cesium and Strontium from Simulated and Actual Hanford 241-AW-101 DSSF Tank Waste*. PNNL-11120, Pacific Northwest National Laboratory, Richland, Washington.

Fiskum, SK, JR Allred, HA Colburn, AM Rovira, MR Smoot, and RA Peterson. 2018. *Multi-Cycle Cesium Ion Exchange Testing Using Spherical Resorcinol-Formaldehyde Resin with Diluted Hanford Tank Waste 241-AP-105*. PNNL-27432, RPT-DFTP-006, Rev. 0, Pacific Northwest National Laboratory, Richland, Washington.

Hamm, LL, T Hang, DJ McCabe, and WD King. 2002. *Preliminary Ion Exchange Modeling for Removal of Cesium from Hanford Waste Using Hydrous Crystalline Silicotitanate Material*. WSRC-TR-2001-00400, Westinghouse Savannah River Company, Aiken, South Carolina.

Harland, CE. 1994. *Ion Exchange: Theory and Practice*. The Royal Society of Chemistry, Cambridge, UK.

Hendrickson, DW, RK Biyani, and MA Beck. 1996. *Hanford Tank Waste Supernatant Cesium Removal Test Report*. WHC-SD-RE-TRP-018, Rev. 0A, Westinghouse Hanford Company, Richland, Washington.

King, W. 2007. *Literature Reviews to Support Ion Exchange Technology Selection for Modular Salt Processing*. WSRC-STI-2007-00609, Washington Savannah River Company, Savannah River Site, Aiken, South Carolina.

Rapko, BM, SI Sinkov, and TG Levitskaia. 2005. "Removal of ¹³⁷Cs from Dissolved Hanford Tank Saltcake by Treatment with IONSIV® IE-911." *Separation Science and Technology* 40(1-3):91-107. doi:10.1081/SS-200041765.

Russell, RL, PP Schonewill, and CA Burns. 2017. *Simulant Development for LAWPS Testing*. RPT-LPIST-001, Rev. 0, PNNL-26165, Pacific Northwest National Laboratory, Richland, Washington.

Walker, DD, DJ Adamson, TD Allen, RW Blessing, WT Boyce, BH Croy, RA Dewberry, DP Diprete, SD Fink, T Hang, JC Hart, MC Lee, JJ Olson, and MJ Whitaker. 1999. *Cesium Removal from Savannah River Site Radioactive Waste Using Crystalline Silicotitanate (IONSIV® IE-911)*. WSRC-TR-99-00308, Rev. 0, Westinghouse Savannah River Company, Aiken, South Carolina.

Appendix A

Column Load and Rinse Data

The measured bed volumes and $\%C/C_0$ values for the three column runs are provided in Table A.1 through Table A.5.

Table A.1. Red Column System, 1.19 BV/h, Cs Load, Feed Displacement, and Water Rinse Results

Lead Column				Lag Column				Feed Displacement and Water Rinse			
BV	$\mu\text{Ci}^{137}\text{Cs}/\text{mL}$	%C/C ₀	DF	BV	$\mu\text{Ci}^{137}\text{Cs}/\text{mL}$	%C/C ₀	DF	BV	$\mu\text{Ci}^{137}\text{Cs}/\text{mL}$	%C/C ₀	DF
8.1	1.22E-7	2.25E-4	443,475	131	1.09E-7	2.00E-4	498,941	Feed displacement			
23.9	1.33E-7	2.46E-4	406,964	214	1.47E-7	2.71E-4	369,583	1.0	6.22E-3	1.14E+1	9
52.2	2.29E-7	4.21E-4	237,604	324	1.55E-7	2.85E-4	351,249	1.9	6.75E-3	1.24E+1	8
80.6	1.36E-6	2.51E-3	39,875	379	8.78E-7	1.62E-3	61,867	2.9	6.64E-3	1.22E+1	8
109	6.69E-6	1.23E-2	8,123	493	1.11E-5	2.05E-2	4,883	4.0	6.10E-3	1.12E+1	9
136	1.86E-5	3.42E-2	2,920	574	4.83E-5	8.89E-2	1,125	5.1	6.32E-3	1.16E+1	9
165	5.57E-5	1.03E-1	975	685	2.41E-4	4.43E-1	226	6.1	3.05E-3	5.62E+0	18
193	1.16E-4	2.14E-1	467	768	5.92E-4	1.09E+0	92	DI water rinse			
221	2.79E-4	5.14E-1	194	882	1.92E-3	3.53E+0	28	0.9	9.71E-4	1.79E+0	56
251	4.92E-4	9.07E-1	110	965	3.26E-3	6.01E+0	17	1.8	3.83E-4	7.05E-1	142
280	8.28E-4	1.53E+0	66	1048	5.42E-3	9.97E+0	10	2.7	2.12E-4	3.89E-1	257
308	1.24E-3	2.28E+0	44	1075	5.67E-3	1.04E+1	10	3.7	1.23E-4	2.27E-1	441
336	1.70E-3	3.14E+0	32					4.6	1.01E-4	1.85E-1	540
365	2.81E-3	5.18E+0	19					5.4	7.18E-5	1.32E-1	757
393	2.63E-3	4.84E+0	21								
421	4.13E-3	7.60E+0	13								
450	5.10E-3	9.39E+0	11								
480	7.11E-3	1.31E+1	7.6								
510	8.42E-3	1.55E+1	6.5								
540	9.59E-3	1.77E+1	5.7								
565	1.09E-2	2.01E+1	5.0								
594	1.20E-2	2.21E+1	4.5								
622	1.59E-2	2.92E+1	3.4								
652	1.85E-2	3.41E+1	2.9								
680	1.88E-2	3.46E+1	2.9								
710	2.16E-2	3.97E+1	2.5								

Table A.2. Red Column System, 1.19 BV/h, Cs Load, Feed Displacement, and Water Rinse Results, Continued

Lead Column				Lag Column				Feed Displacement and Water Rinse			
BV	$\mu\text{Ci}^{137}\text{Cs}/\text{mL}$	$\%C/C_0$	DF	BV	$\mu\text{Ci}^{137}\text{Cs}/\text{mL}$	$\%C/C_0$	DF	BV	$\mu\text{Ci}^{137}\text{Cs}/\text{mL}$	$\%C/C_0$	DF
736	2.46E-2	4.53E+1	2.2								
766	2.43E-2	4.48E+1	2.2								
795	2.63E-2	4.84E+1	2.1								
825	2.67E-2	4.91E+1	2.0								
853	3.36E-2	6.18E+1	1.6								
882	3.27E-2	6.01E+1	1.7								
913	3.67E-2	6.75E+1	1.5								
942	3.77E-2	6.95E+1	1.4								
968	4.09E-2	7.53E+1	1.3								
999	3.95E-2	7.28E+1	1.4								
1028	4.11E-2	7.57E+1	1.3								
1057	4.36E-2	8.03E+1	1.2								
1084	4.25E-2	7.82E+1	1.3								
1112	4.42E-2	8.13E+1	1.2								

BV = bed volume; DI = deionized; DF = decontamination factor; $C_0 = 0.0543 \mu\text{Ci}^{137}\text{Cs}/\text{mL}$.

Table A.3. Blue Column System, 1.99 BV/h, Cs Load, Feed Displacement, and Water Rinse Results

Lead Column				Lag Column				Feed Displacement and Water Rinse			
BV	$\mu\text{Ci}^{137}\text{Cs}/\text{mL}$	%C/C ₀	DF	BV	$\mu\text{Ci}^{137}\text{Cs}/\text{mL}$	%C/C ₀	DF	BV	$\mu\text{Ci}^{137}\text{Cs}/\text{mL}$	%C/C ₀	DF
15	1.62E-7	3.06E-4	326,517	41	1.69E-7	3.19E-4	313,967	Feed displacement			
42	3.77E-7	7.12E-4	140,403	177	1.33E-7	2.51E-4	398,773	1.0	1.15E-2	2.17E+1	5
89	1.13E-5	2.13E-2	4,705	308	1.55E-6	2.93E-3	34,173	2.0	1.09E-2	2.05E+1	5
135	7.08E-5	1.34E-1	747	351	4.85E-6	9.17E-3	10,911	2.9	1.20E-2	2.27E+1	4
181	2.93E-4	5.54E-1	180	393	1.25E-5	2.36E-2	4,234	3.9	1.30E-2	2.46E+1	4
228	7.00E-4	1.32E+0	76	440	3.23E-5	6.11E-2	1,638	4.9	1.17E-2	2.22E+1	5
270	1.38E-3	2.61E+0	38	485	6.77E-5	1.28E-1	782	5.9	4.65E-3	8.78E+0	11
315	2.11E-3	3.99E+0	25	531	1.21E-4	2.29E-1	437	DI water rinse			
362	3.98E-3	7.52E+0	13	576	2.29E-4	4.32E-1	232	1.0	2.05E-3	3.87E+0	26
382	4.66E-3	8.81E+0	11	596	2.92E-4	5.52E-1	181	2.0	7.05E-4	1.33E+0	75
403	5.88E-3	1.11E+1	9.0	618	4.14E-4	7.81E-1	128	3.0	2.99E-4	5.65E-1	177
430	7.18E-3	1.36E+1	7.4	663	5.60E-4	1.06	94	4.0	1.84E-4	3.48E-1	287
452	7.37E-3	1.39E+1	7.2	757	8.70E-4	1.64	61	5.0	1.21E-4	2.28E-1	439
480	1.01E-2	1.91E+1	5.2	805	1.30E-3	2.46	41	6.0	9.65E-5	1.82E-1	549
499	9.90E-3	1.87E+1	5.3	856	2.67E-3	5.05	20				
527	1.22E-2	2.30E+1	4.3	945	4.27E-3	8.07	12				
547	1.24E-2	2.35E+1	4.3	1039	6.64E-3	12.5	8				
575	1.45E-2	2.73E+1	3.7	1086	8.47E-3	16.0	6				
594	1.56E-2	2.94E+1	3.4	1134	9.31E-3	17.6	6				
624	1.70E-2	3.20E+1	3.1	1142	9.51E-3	18.0	6				
649	1.65E-2	3.12E+1	3.2								
671	2.16E-2	4.07E+1	2.5								
684	1.92E-2	3.63E+1	2.8								
718	2.45E-2	4.63E+1	2.2								
731	2.37E-2	4.47E+1	2.2								
795	2.43E-2	4.58E+1	2.2								
846	2.92E-2	5.52E+1	1.8								
883	2.90E-2	5.48E+1	1.8								

Table A.4. Blue Column System, 1.99 BV/h, Cs Load, Feed Displacement, and Water Rinse Results, Continued

Lead Column				Lag Column				Feed Displacement and Water Rinse			
BV	$\mu\text{Ci } ^{137}\text{Cs/ mL}$	$\%C/C_0$	DF	BV	$\mu\text{Ci } ^{137}\text{Cs/ mL}$	$\%C/C_0$	DF	BV	$\mu\text{Ci } ^{137}\text{Cs/ mL}$	$\%C/C_0$	DF
938	3.04E-2	5.75E+1	1.7								
974	3.45E-2	6.52E+1	1.5								
1036	3.91E-2	7.38E+1	1.4								
1069	3.95E-2	7.46E+1	1.3								
1134	4.20E-2	7.92E+1	1.3								
1184	4.73E-2	8.94E+1	1.1								
1194	4.72E-2	8.91E+1	1.1								

BV = bed volume; DI = deionized; DF = decontamination factor; $C_0 = 0.0530 \mu\text{Ci } ^{137}\text{Cs/ mL}$.

Table A.5. Green Column System, 4.56 BV/h, Cs Load, Feed Displacement, and Water Rinse Results

Lead Column				Lag Column			
BV	$\mu\text{Ci}^{137}\text{Cs}/\text{mL}$	%C/C ₀	DF	BV	$\mu\text{Ci}^{137}\text{Cs}/\text{mL}$	%C/C ₀	DF
12	9.20E-5	1.65E-1	606	12	6.86E-5	1.23E-1	812
37	3.52E-5	6.33E-2	1,581	36	5.10E-7	9.15E-4	109,258
96	4.98E-4	8.95E-1	112	94	5.88E-7	1.06E-3	94,656
145	1.60E-3	2.86E+0	35	142	3.35E-6	6.01E-3	16,652
205	3.54E-3	6.36E+0	16	201	1.87E-5	3.36E-2	2,976
255	5.67E-3	1.02E+01	10	250	5.60E-5	1.00E-1	995
314	7.92E-3	1.42E+01	7.0	309	1.56E-4	2.79E-1	358
364	1.14E-2	2.05E+01	4.9	357	3.48E-4	6.24E-1	160
429	1.41E-2	2.53E+01	4.0	422	6.58E-4	1.18E+0	85
471	1.76E-2	3.16E+01	3.2	462	9.99E-4	1.79E+0	56
540	1.89E-2	3.40E+01	2.9	530	1.66E-3	2.97E+0	34
589	2.31E-2	4.14E+01	2.4	578	2.28E-3	4.10E+0	24
641	2.58E-2	4.63E+01	2.2	629	3.13E-3	5.61E+0	18
691	2.76E-2	4.95E+01	2.0	678	4.15E-3	7.46E+0	13
758	3.01E-2	5.40E+01	1.9	744	5.17E-3	9.28E+0	11
802	3.26E-2	5.84E+01	1.7	787	7.41E-3	1.33E+1	7.5
869	3.37E-2	6.05E+01	1.7	854	6.72E-3	1.21E+1	8.3
911	3.85E-2	6.91E+01	1.4	894	9.85E-3	1.77E+1	5.7
981	4.07E-2	7.30E+01	1.4	964	1.10E-2	1.97E+1	5.1
1020	3.84E-2	6.89E+01	1.5	1002	1.24E-2	2.23E+1	4.5
1087	3.89E-2	6.98E+01	1.4	1067	1.43E-2	2.57E+1	3.9
1125	4.44E-2	7.97E+01	1.3	1105	1.57E-2	2.81E+1	3.6

BV = bed volume; DI = deionized; DF = decontamination factor; C₀ = 0.0557 $\mu\text{Ci}^{137}\text{Cs}/\text{mL}$.

No feed displacement or water rinse was applied because the columns were accidentally pumped dry after feed.

Distribution

**No. of
Copies**

**No. of
Copies**

4 Washington River Protection Solutions

ST Arm (PDF)
KA Colosi (PDF)
MR Landon (PDF)
JG Reynolds (PDF)

10 Pacific Northwest National Laboratory

SK Fiskum (PDF)
JR Allred (PDF)
HA Colburn (PDF)
M Fountain (PDF)
RA Peterson (PDF)
AM Rovira (PDF)
SN Schlahta (PDF)
MR Smoot (PDF)
DM Wellman (PDF)
Information Release (PDF)



**Pacific
Northwest**
NATIONAL LABORATORY

www.pnnl.gov

902 Battelle Boulevard
P.O. Box 999
Richland, WA 99352
1-888-375-PNNL (7665)

U.S. DEPARTMENT OF
ENERGY